Imperial College London

Upstream Influence Leading to Discontinuous Solutions of the Boundary-Layer Equations

by

Ali Haseeb Khalid

CID**00467434**

supervised by

Prof. Anatoly I. Ruban

Department of Mathematics

Faculty of Engineering,

Department of Aeronautics

September 2010

Acknowledgements

I owe my deepest gratitude to my supervisor, Professor Anatoly Ruban, who kindly provided this project for me, along with encouragement and support, allowing me to delve into a significant area of fluid dynamics and mathematics.

An honourable mention goes to my family and friends for their understanding and support during my studies.

I would also like to take this opportunity to thank the Royal Aeronautical Society (RAeS) for providing me with a scholarship and making these studies possible.

Abstract

This project looks back at the work and ideas of some fluid dynamists from the 20th century. Revisiting the boundary-layer/shockwave interaction and upstream influence, first discovered in scientific experiments during the late 1930's and early 1940's, we attempt to seek a prediction for the pressure distribution when the shock wave moves along the boundary-layer, or equivalently, when the boundary is in motion.

Working with simplified boundary-layer equations, deduced using the method of *matched asymptotic expansions*, and under the assumption that the pressure acting upon the boundary-layer experiences a sharp variation (increase) in a region which is small as compared to the size of the body placed in the flow, the classical *triple-deck equations* are achieved. Using linearised theory and by seeking a particular solution of the derived equations, we analyse the upstream influence for an upstream and downstream moving boundary.

In the case of a stationary and downstream moving boundary, the equations are solved analytically via methods of *complex analysis*. For the case of the boundary moving upstream, the solution is found in an integral form, which is subsequently calculated numerically. This provides some interesting results of the pressure distribution in the vicinity of the *interaction region*, which may lead to a discontinuous solution.

Contents

1 Introduction

Separated and high-speed flows have been, and still are subjects of high interest , posing particularly interesting challenges for both mathematicians and engineers alike. During the late 19^{th} to early 20^{th} century, the problem of flow separation was a topic at the top of many researchers interests. Many attempts to develop theoretical models were made, the first of which was due to Helmholtz (1868), for flow past a perpendicular plate. Another model due to Kirchhoff (1869) was more flexible as it accounted for varying body shapes, namely Levi-Civita (1907) applied this model to the flow past a circular cylinder. These models, formulated using classical inviscid flow theory, lead to a conclusion that the Euler equations allow for a family of solutions where the separation point remains a free parameter.

In 1904, it was Prandtl who was the first to identify that the non-uniqueness (due to separation point) could be resolved through the specific behaviour of the boundary-layer. Prandtl's boundary-layer theory consists of two key assumptions which state:

> *(i) For large Reynolds number flows, the viscosity is negligible in the majority of the flow, where the Euler equations are applicable. Essentially, the flow can be considered inviscid.*
>
> *(ii) In the thin layer in the vicinity of the boundary, viscous terms are important as the inertia terms, no matter how large the Reynolds number. Across this thin layer the slip velocity is reduced to zero.*

This essentially means the fluid immediately adjacent to the boundary surface, sticks to the surface, and that the viscous effects take place in a thin layer called the *boundary-layer*. The specific behaviour of the boundary-layer depends on the pressure gradients along the boundary surface. If the pressure decreases downstream (favourable pressure gradient), then the boundary-layer remains attached to the boundary surface. However, if the pressure increases downstream in the direction of the flow (adverse pressure gradient), the boundary-layer separates from the boundary surface. This separation was explained due to the motion of the particles in the boundary-layer. Small increases in pressure downstream could cause particles near the boundary surface to slow and turn back causing flow reversal and recirculation, which originates at the point of separation.

Prandtl's original paper, which he presented in Heidelberg at the Third International Mathematics Congress was very short, however, one which would revolutionaries fluid dynamics. Now, boundary-layer theory is an integral part of fluid dynamics, especially when studying separation and high Reynolds number flows, which cover a wide range of natural flows and many of those in engineering applications, namely aerodynamics.

Many flows of considerable interest are also compressible and supersonic, for example, flow over the wing of a supersonic aircraft. In supersonic flows, shock waves can develop, which abruptly alter the characteristics of the flow as they propagate through the medium.

This report will take a mathematical approach to a very specific problem, namely shock wave/boundary-layer interaction. This requires the understanding of the fluid flow in the vicinity of the boundary and the *interaction region*, where the shock wave impinges on the boundary-layer. For the purpose of this report we will assume the boundary-layer is laminar.

1.1 Historic overview leading to upstream influence and asymptotic theory

The classical boundary-layer theory, as presented by Prandtl, was a mean to understand and predict separation which was based on a hierarchical approach. Here, the outer inviscid flow should be calculated first, ignoring the existence of the boundary-layer, after which we should consult boundary-layer analysis. However, Landau & Lifshitz (1944) highlighted a problem with such an approach, which would lead to a mathematical contradiction. They showed that the skin friction, which can be defined as

$$\tau_w = \mu \left.\frac{\partial u}{\partial y}\right|_{y=0}, \tag{1.1}$$

produced by the boundary-layer decreased as separation is approached, however, simultaneously the velocity component normal to the boundary experiences unbounded growth. Near the point of separation, a singularity occurs, which was of Landu & Lifschitz main interest. Goldstein (1948) produced an in-depth mathematical analysis of the boundary-layer equations in the vicinity of the point of separation and zero skin friction. Henceforth, the singularity is known as the Goldstein singularity. This study was of great importance as Goldstein demonstrated that the singularity at separation inhibits the solution of the boundary-layer equations after the point of zero skin friction.

During Goldstein's discovery, many experimentalists were making ground breaking discoveries of their own regarding separated flows. One physical situation which warranted research efforts, was the effect of a shock wave impinging on a boundary-layer in a supersonic flow. This was because of the upstream influence through the boundary-layer which was evident prior to separation. A review of many of the experimental efforts can be found in Chapman *et al.* (1956).

To produce the effect of a shock wave impinging on a boundary-layer, the likes of F. Barry and E. Neumann designed apparatus for experiments which were replicated durning the forties and fifties. For the purpose of this report, to gain some understanding of the experimental layout, let us consider the simple model of a test section shown in Figure 1.1 below.

Here the shape of the smooth "wedge" body, above the plate on which the boundary-layer develops, is described by

$$y = -\frac{\alpha_0}{2}\left(x + \sqrt{x^2 + d^2}\right) + constant. \tag{1.2}$$

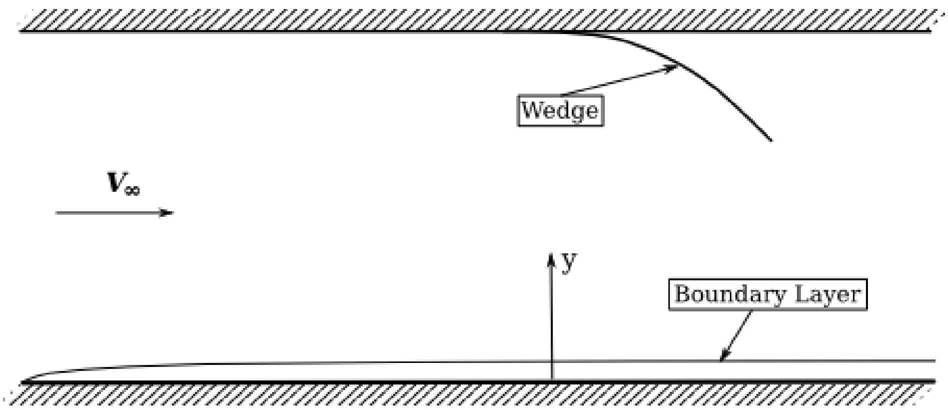

Figure 1.1*:* Example of experimental layout with smooth body or wedge above the boundary-layer along a flat plate.

If $d = 0$ then the body shape becomes a simple straight wedge, which is often used in experiments to form shock waves in supersonic wind tunnels and α_0 is a positive real quantity which regulates the shock strength. Reasoning behind the choice of such a body shape is due to the different effects of pressure variation which can be achieved on the boundary-layer. For instance, if $d \neq 0$ then the pressure would vary smoothly along the boundary-layer, whereas if $d = 0$, there would be a spike in pressure, where the shock wave would impinge on the boundary-layer. The smooth body or wedge produces a weak shock which impinges on the boundary-layer as shown in Figure 1.2 below.

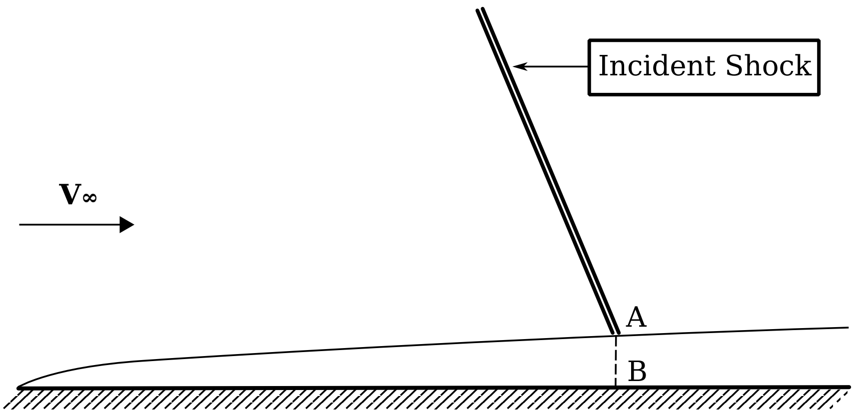

Figure 1.2*:* Shock wave impinging upon the boundary-layer on a flat plate.

To describe the effects of the flow behaviour using classical boundary-layer theory, where firstly the existence of the boundary-layer is neglected to leading order and the outer flow is considered inviscid where we apply the Euler equations. One must note, at supersonic speed, the Euler equations are hyperbolic, thus they do not allow for the propagation of perturbations upstream, i.e. perturbations only move in the downstream direction in the *Mach cone.* Hence, it is expected that the flow upstream of the shock remains uniform and undisturbed. After this, we turn to the boundary-layer equations which describe the flow in the boundary-layer. For a given pressure, the boundary-layer equations are parabolic and also inhibit any propagation of perturbations upstream of the corss-section AB, where the shock wave meets the boundary-layer at A.

However, what experimentalists discovered was contrary to what a theoretician may conclude, as described above. The experimentalists (such as Liepmann *et al.* (1949) and others such as R. Chapman and J. Ackeret) showed in scenarios as depicted in Figure 1.2, the boundary-layer separated from the plate surface upstream of the incident shock wave and pressure perturbations were able to propagate far upstream through the boundary-layer, past the point of separation; distances much larger than the thickness of the boundary-layer itself. The boundary-layer separation can be seen in Figure 1.3. From the experiments, it could be physically explained, that the pressure increase upstream of the point of separation would cause the streamlines to deviate from the wall near the plate, causing a secondary shock. This characteristic is depicted in Figure 1.4, and is termed the λ-shock structure, as described by Liepmann *et al.* (1949) for a laminar boundary-layer. Between the surface and the separated boundary-layer is a region of stagnant or slowly eddying fluid.

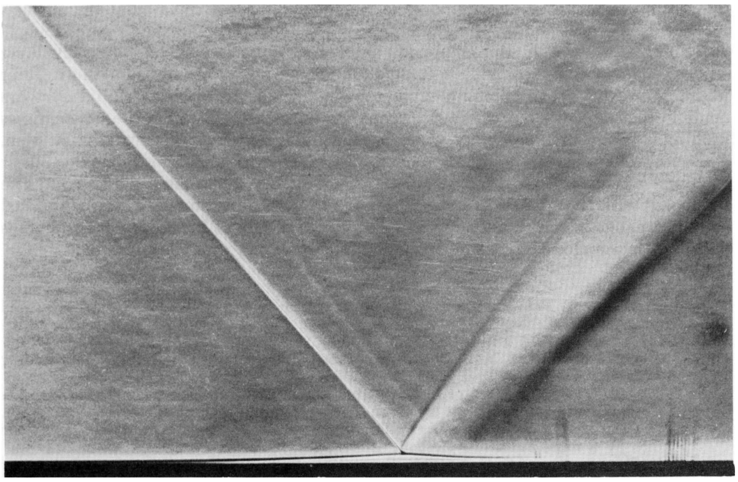

Figure 1.3*:* Shock wave impinging upon the boundary-layer, visualisation by Liepmann *et al.* (1949).

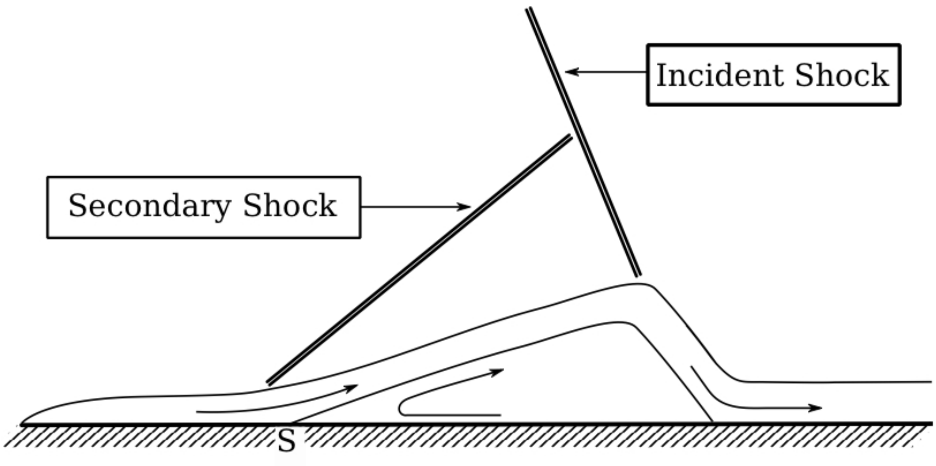

Figure 1.4*:* Schematic representation of the λ-structure of the impinging and secondary shocks.

A paper written by Oswatitsch & Wieghardt (1948) first described the interaction between the inviscid outer flow and the boundary-layer as the cause behind the upstream influence. The impinging shock wave is simply a means to the beginning of a self sustained process which leads to the separation of the boundary-layer from the plate surface. This physical phenomenon can be described as follows. Assume that there is an increase in pressure at the outer edge of the boundary-layer down stream. This leads to the deceleration of fluid particles in the boundary-layer, as pressure perturbations can penetrate into the boundary-layer. This leads to deviation of streamlines from the surface, which in turn leads to an increase in pressure in the external supersonic flow due to the displacement of the boundary-layer and the process repeats. Chapman *et al.* (1956) eluded to this process as *free-interaction.*

Asymptotic theory of the free-interaction and separation of the boundary-layer have been developed by K. Stewartson & G. Williams (1969) and Y. Nieland (1969) independently. Both of these papers which consist of theories that will be utilised later, stem from the efforts of S. Kaplun and his work on matched asymptotic expansions and the formation of the matching region, of which much of the development is due to P. Lagerstrom.

One can see the importance experiments hold in this field of study, as with many other areas of study. Discovering physical phenomena and understanding the physical aspects are key before theoretical and rigorous mathematical models can be developed, for example the linearised theory of Lighthill (1953, 2000), to describe such phenomenon as boundary-layer/shock wave interaction and upstream influence. Many papers have been written in the past dedicated to shock wave/boundary-layer interaction from both an experimental and analytical stance, which have invariably concluded that the boundary-layer forms a critical factor of the overall flow. The majority of the efforts conducted in the past consider a fixed boundary, however, in this report we will see how we can take the concepts developed and apply them to the case in which the boundary is in motion.

1.2 Formulation of Shock Wave/Boundary-Layer Interaction

1.2.1 The governing equations

In order to proceed, the flow layout as described in Figure 1.2 is considered, where compressible viscous fluid is flowing past a flat plate in which an oblique shock wave impinges on a fully developed boundary-layer. To begin we will assume the fluid motion is steady and two dimensional. We will also assume the gas can be treated as perfect. The motion is governed by the Navier-Stokes equations as given below.[1]

$$\hat{\rho}\left(\hat{u}\frac{\partial \hat{u}}{\partial \hat{x}} + \hat{v}\frac{\partial \hat{u}}{\partial \hat{y}}\right) = -\frac{\partial \hat{p}}{\partial \hat{x}} + \frac{\partial}{\partial \hat{x}}\left[\hat{\mu}\left(\frac{4}{3}\frac{\partial \hat{u}}{\partial \hat{x}} - \frac{2}{3}\frac{\partial \hat{v}}{\partial \hat{y}}\right)\right] + \frac{\partial}{\partial \hat{y}}\left[\hat{\mu}\left(\frac{\partial \hat{u}}{\partial \hat{y}} + \frac{\partial \hat{v}}{\partial \hat{x}}\right)\right], \tag{1.3}$$

[1]The reader is referred to a book by D. Rogers (1992) for a rigorous derivation of the governing equation for viscous compressible fluid.

$$\hat{\rho}\left(\hat{u}\frac{\partial \hat{v}}{\partial \hat{x}}+\hat{v}\frac{\partial \hat{v}}{\partial \hat{y}}\right)=-\frac{\partial \hat{p}}{\partial \hat{x}}+\frac{\partial}{\partial \hat{x}}\left[\hat{\mu}\left(\frac{4}{3}\frac{\partial \hat{v}}{\partial \hat{y}}-\frac{2}{3}\frac{\partial \hat{u}}{\partial \hat{x}}\right)\right]+\frac{\partial}{\partial \hat{x}}\left[\hat{\mu}\left(\frac{\partial \hat{u}}{\partial \hat{y}}+\frac{\partial \hat{v}}{\partial \hat{x}}\right)\right], \tag{1.4}$$

$$\frac{\partial \hat{\rho}\hat{u}}{\partial \hat{x}}+\frac{\partial \hat{\rho}\hat{v}}{\partial \hat{y}}=0, \tag{1.5}$$

$$\hat{\rho}\left(\hat{u}\frac{\partial \hat{h}}{\partial \hat{x}}+\hat{v}\frac{\partial \hat{h}}{\partial \hat{y}}\right)=\hat{u}\frac{\partial \hat{p}}{\partial \hat{x}}+\hat{v}\frac{\partial \hat{p}}{\partial \hat{y}}+\frac{1}{Pr}\left[\frac{\partial}{\partial \hat{x}}\left(\hat{\mu}\frac{\partial \hat{h}}{\partial \hat{x}}\right)+\frac{\partial}{\partial \hat{y}}\left(\hat{\mu}\frac{\partial \hat{h}}{\partial \hat{y}}\right)\right]+$$
$$+\hat{\mu}\left(\frac{4}{3}\frac{\partial \hat{u}}{\partial \hat{x}}-\frac{2}{3}\frac{\partial \hat{v}}{\partial \hat{y}}\right)\frac{\partial \hat{u}}{\partial \hat{x}}+\hat{\mu}\left(\frac{4}{3}\frac{\partial \hat{v}}{\partial \hat{y}}-\frac{2}{3}\frac{\partial \hat{u}}{\partial \hat{x}}\right)\frac{\partial \hat{v}}{\partial \hat{y}}+\hat{\mu}\left(\frac{\partial \hat{u}}{\partial \hat{y}}+\frac{\partial \hat{v}}{\partial \hat{x}}\right)^2, \tag{1.6}$$

$$\hat{h}=\frac{\gamma}{\gamma-1}\frac{\hat{p}}{\hat{\rho}}. \tag{1.7}$$

Here, equation (1.3) and (1.4) represent the x and y momentum equations respectively, which together with the continuity equation (1.5), form what are known as the Navier-Stokes equations. However since the flow is also compressible we have the energy equation (1.6) and the equation of state (1.7). In the equations presented, Pr represents the Prandtl number, which is typically defined as

$$Pr=\frac{\text{viscous diffusion}}{\text{thermal diffusion}}.$$

To study the flow a Cartesian co-ordinate system is used where $\hat{x}$ is measured along the flat plate and $\hat{y}$ perpendicular. Here *hat* will denote dimensional variables, where the quantities in the above equations are the velocity components $\hat{u}$ and $\hat{v}$ in the $\hat{x}$ and $\hat{y}$ directions respectively, density $\hat{\rho}$, pressure $\hat{p}$, dynamic viscosity $\hat{\mu}$ and enthalpy $\hat{h}$. Here γ denotes the gas constant given by the ratio of the specific heats of the gas. The density, pressure, viscosity and velocity of the unperturbed upstream flow are ρ_∞, p_∞, μ_∞ and V_∞ respectively. Here the suffix ∞ denotes conditions at an infinite distance upstream.

The distance from the leading edge of the plate to the point B (see Figure 1.2), where the shockwave impinges on the boundary-layer is denoted by L, with which we shall non-dimensionalise the governing equations. It is justifiable to assume the boundary-layer is fully developed at $x=L$. The following non-dimensional variables are introduced.

$$\begin{aligned}
&\hat{x}=Lx, &&\hat{y}=Ly, &&\hat{u}=V_\infty u, &&\hat{v}=V_\infty v,\\
&\hat{\rho}=\rho_\infty\rho, &&\hat{p}=p_\infty+\rho_\infty V_\infty^2 p, &&\hat{\mu}=\mu_\infty, &&\hat{h}=V_\infty^2 h.
\end{aligned} \tag{1.8}$$

Hence, substituting the non-dimensional variables into equations (1.3)-(1.7) and rearranging, the following non-dimensional governing equations are achieved.

$$\rho\left(u\frac{\partial u}{\partial x}+v\frac{\partial u}{\partial y}\right)=-\frac{\partial p}{\partial x}+\frac{1}{Re}\left\{\frac{\partial}{\partial x}\left[\mu\left(\frac{4}{3}\frac{\partial u}{\partial x}-\frac{2}{3}\frac{\partial v}{\partial y}\right)\right]+\frac{\partial}{\partial y}\left[\mu\left(\frac{\partial u}{\partial y}+\frac{\partial v}{\partial x}\right)\right]\right\}, \tag{1.9}$$

$$\rho\left(u\frac{\partial v}{\partial x}+v\frac{\partial v}{\partial y}\right)=-\frac{\partial p}{\partial y}+\frac{1}{Re}\left\{\frac{\partial}{\partial x}\left[\mu\left(\frac{4}{3}\frac{\partial v}{\partial y}-\frac{2}{3}\frac{\partial u}{\partial x}\right)\right]+\frac{\partial}{\partial x}\left[\mu\left(\frac{\partial u}{\partial y}+\frac{\partial v}{\partial x}\right)\right]\right\}, \tag{1.10}$$

$$\frac{\partial \rho u}{\partial x}+\frac{\partial \rho v}{\partial y}=0, \tag{1.11}$$

$$\rho\left(u\frac{\partial h}{\partial x}+v\frac{\partial h}{\partial y}\right)=u\frac{\partial p}{\partial x}+v\frac{\partial p}{\partial y}+\frac{1}{Re}\left\{\frac{1}{Pr}\left[\frac{\partial}{\partial x}\left(\mu\frac{\partial h}{\partial x}\right)+\frac{\partial}{\partial y}\left(\mu\frac{\partial h}{\partial y}\right)\right]+\right.$$
$$\left.+\mu\left(\frac{4}{3}\frac{\partial u}{\partial x}-\frac{2}{3}\frac{\partial v}{\partial y}\right)\frac{\partial u}{\partial x}+\mu\left(\frac{4}{3}\frac{\partial v}{\partial y}-\frac{2}{3}\frac{\partial u}{\partial x}\right)\frac{\partial v}{\partial y}+\mu\left(\frac{\partial u}{\partial y}+\frac{\partial v}{\partial x}\right)^2\right\}, \tag{1.12}$$

$$h=\frac{\gamma}{\gamma-1}\frac{p}{\rho}+\frac{1}{M_\infty^2(\gamma-1)}\frac{1}{\rho}. \tag{1.13}$$

To represent the difference in pressure which is associated with the existence of the oblique shock wave, produced by an obstacle above the boundary-layer, the pressure p in the equations above can be written as a follows

$$p(x,y)=p_0(x)+\mathbb{P}(x,y). \tag{1.14}$$

Here $\mathbb{P}$ is considered as the induced pressure distribution as a result of an imposed pressure p_0, which is a step function defined as

$$p_0(x)=\begin{cases}\alpha_0 & \text{for all } x>1\\ 0 & \text{for all } x<1\end{cases}, \tag{1.15}$$

where α_0 is a quantity which regulates the shock strength and relates to the angle of the wedged body above the boundary-layer.

In equations (1.9)-(1.11), there appears an important non-dimensional parameter Re, known as the Reynolds number, which is defined as

$$Re=\frac{\rho_\infty V_\infty L}{\mu_\infty},$$

The asymptotic analysis of the Navier-Stokes equations (1.9) - (1.13) shall be conducted under the assumption $Re\to\infty$. Also, M_∞ denotes the free stream Mach number, which we will assume to be greater than one as we are considering a supersonic flow. Here the Mach number is defined as

$$M_\infty=\frac{V_\infty}{a_\infty},$$

where a_∞ is the free stream speed of sound, defined as

$$a_\infty=\sqrt{\frac{\gamma p_\infty}{\rho_\infty}}.$$

2 Preliminaries

Here we consider the asymptotic analysis in the boundary-layer, leading to the triple-deck structure. For an understanding behind the method of matched asymptotic expansions, see appendix B.

2.1 Asymptotic analysis upstream of separation

As mentioned earlier, there are two identified regions; one being the outer inviscid flow and the other known as the boundary-layer. In the inviscid region we have the length scale L (as was denoted earlier) in both directions of space. The flow in this region is uniform, where the presence of the boundary-layer can cause perturbations of order $O(Re^{-1/2})$. In the boundary-layer, two length scales are required, one along the plate surface which is as before, and an appropriate scale perpendicular to the surface.

Since the flow and the boundary-layer prior to the shock impingement plays a roll in the overall interaction procedure, we will first consider the boundary-layer upstream of this point. Thus, we begin the asymptotic analysis of the boundary-layer on the following limit procedure

$$x = O(1), \qquad Y = \frac{y}{Re^{-1/2}} = O(1), \qquad Re \to \infty. \tag{2.1}$$

The corresponding solution of the Navier-Stokes equations (1.9)-(1.13) may be expressed in the following asymptotic expansions.

$$\begin{aligned}
u(x,y;Re) &= U_0(x,Y) + Re^{-1/2}U_1(x,Y) + Re^{-1}U_2(x,Y) + \dots, \\
v(x,y;Re) &= Re^{-1/2}V_1(x,Y) + Re^{-1}V_2(x,Y) + \dots, \\
\mathbb{P}(x,y;Re) &= Re^{-1/2}P_1(x,Y) + Re^{-1}P_2(x,Y) + \dots, \\
\rho(x,y;Re) &= \rho_0(x,Y) + Re^{-1/2}\rho_1(x,Y) + Re^{-1}\rho_2(x,Y) + \dots, \\
\mu(x,y;Re) &= \mu_0(x,Y) + Re^{-1/2}\mu_1(x,Y) + Re^{-1}\mu_2(x,Y) + \dots, \\
h(x,y;Re) &= h_0(x,Y) + Re^{-1/2}h_1(x,Y) + Re^{-1}h_2(x,Y) + \dots.
\end{aligned} \tag{2.2}$$

Substituting equations (2.2) in to equations (1.9)-(1.13) yields the following set of equations to leading order.[2]

$$\rho_0 U_0 \frac{\partial U_0}{\partial x} + \rho_0 V_0 \frac{\partial U_0}{\partial Y} = \frac{\partial}{\partial Y}\left(\mu_0 \frac{\partial U_0}{\partial Y}\right), \tag{2.3a}$$

$$\frac{\partial P_1}{\partial Y} = 0, \tag{2.3b}$$

$$\frac{\partial}{\partial x}(\rho_0 U_0) + \frac{\partial}{\partial Y}(\rho_0 V_0) = 0, \tag{2.3c}$$

$$\rho_0 U_0 \frac{\partial h_0}{\partial x} + \rho_0 V_0 \frac{\partial h_0}{\partial Y} = \frac{1}{Pr}\frac{\partial}{\partial Y}\left(\mu_0 \frac{\partial h_0}{\partial Y}\right) + \mu_0 \left(\frac{\partial U_0}{\partial Y}\right)^2, \tag{2.3d}$$

[2]Note, upstream of the shock, $p(x,y)$ is simply $\mathbb{P}(x,y)$.

$$h_0 = \frac{1}{M_\infty^2(\gamma-1)\rho_0}. \tag{2.3e}$$

These equations are those of classical boundary-layer theory, in particular, these represent the steady compressible boundary-layer equations and are parabolic. These equations should be solved with the following conditions

$$U_0 = 1, \quad h_0 = \frac{1}{M_\infty^2(\gamma-1)} \qquad \text{at} \qquad x = 0, \quad Y \in [0, \infty), \tag{2.4}$$

$$U_0 = 1, \quad h_0 = \frac{1}{M_\infty^2(\gamma-1)} \qquad \text{at} \qquad Y = \infty, \quad x \in [0, \infty), \tag{2.5}$$

$$U_0 = 0, \quad V_0 = 0 \qquad \text{at} \qquad Y = 0, \quad x \in [0, 1]. \tag{2.6}$$

Here, (2.4) represents the condition at the leading edge of the flat plate, (2.5) represents the condition at the outer edge of the boundary-layer and (2.6) represents the no slip condition on the flat plate. We also require a thermal condition. Assuming the plate (boundary) is thermally isolated, we will have

$$\frac{\partial h_0}{\partial Y} = 0 \qquad \text{at} \qquad Y = 0, \quad x \in [0, 1]. \tag{2.7}$$

Equations (2.3) together with conditions (2.4)-(2.7) form a boundary-value problem which admits self similar solutions. Now, if we assume the solution to be smooth as the cross section AB is approached (see Figure 1.2), then the sought functions may be represented in the form of Taylor expansions as follows

$$\left.\begin{aligned} U_0(x,Y) &= U_{00}(Y) - sU_{01}(Y) + \dots \\ \rho_0(x,Y) &= \rho_{00}(Y) - s\rho_{01}(Y) + \dots \\ \mu_0(x,Y) &= \mu_{00}(Y) - s\mu_{01}(Y) + \dots \\ h_0(x,Y) &= h_{00}(Y) - sh_{01}(Y) + \dots \end{aligned}\right\} \quad \text{as} \qquad s = x - 1 \to 0^-, \tag{2.8}$$

where the leading order terms have the following characteristics

$$\left.\begin{aligned} U_{00}(Y) &= \lambda Y + \dots \\ \rho_{00}(Y) &= \rho_w + \dots \\ \mu_{00}(Y) &= \mu_w + \dots \\ h_{00}(Y) &= h_w + \dots \end{aligned}\right\} \quad \text{as} \qquad Y \to 0. \tag{2.9}$$

Here, λ, ρ_w, μ_w and h_w are positive constants of dimensionless skin friction, density, dynamic viscosity and enthalpy at the boundary surface.

2.2 Inspection analysis of free-interaction

2.2.1 Main boundary-layer

Now let us consider an order of magnitude analysis of the region in which the shock wave impinges on the boundary-layer. Let us assume the shock wave is weak and there is a rise in pressure of $\Delta p \ll 1$ at the outer edge of the boundary-layer (point A). Also, we assume the distance over which the pressure rise occurs is small, i.e. $\Delta x \ll 1$, say. We expect this increase of pressure to cause a deceleration of the fluid particles. Since the convective terms in the momentum equation describe the acceleration or deceleration of the fluid particles, to estimate the change in velocity, Δu, we compare the first convective term in (1.9) with the pressure term, as given in the balance below[3]

$$\rho u \frac{\partial u}{\partial x} \sim \frac{\partial p}{\partial x}. \tag{2.10}$$

Since the variations are very small, we can represent the velocity and density with the initial leading order terms as given in equation (2.8). Approximating the derivatives as small variations we see

$$\rho_{00} U_{00} \frac{\Delta u}{\Delta x} \sim \frac{\Delta p}{\Delta x}, \tag{2.11}$$

which yields

$$\Delta u \sim \frac{\Delta p}{\rho_{00} U_{00}}, \tag{2.12}$$

and since the leading order terms are order one quantities everywhere in the boundary-layer (except in the viscous sublayer close to the boundary) we have

$$\Delta u \sim \Delta p. \tag{2.13}$$

Now, turning to the energy equation (1.11), comparing the convective terms and the pressure terms we see

$$\rho_{00} U_{00} \frac{\Delta h}{\Delta x} \sim U_{00} \frac{\Delta p}{\Delta x}, \tag{2.14}$$

hence, we obtain

$$\Delta h \sim \Delta p. \tag{2.15}$$

If we consider the equation of state (1.13), and differentiate with respect to x we have

$$\frac{\partial h}{\partial x} = \frac{\gamma}{(\gamma-1)\rho^2}\left(\frac{\partial p}{\partial x} - \frac{\partial \rho}{\partial x}\right) - \frac{1}{M_\infty^2(\gamma-1)\rho^2}\frac{\partial \rho}{\partial x}, \tag{2.16}$$

approximating the derivatives as before and representing density with leading order terms from (2.8) we have

$$\frac{\Delta h}{\Delta x} \sim \frac{\gamma}{(\gamma-1)\rho_{00}^2}\left(\frac{\Delta p}{\Delta x} - \frac{\Delta \rho}{\Delta x}\right) - \frac{1}{M_\infty^2(\gamma-1)\rho_{00}^2}\frac{\Delta \rho}{\Delta x}. \tag{2.17}$$

Since $\Delta h \sim \Delta p$ and $\rho_{00} \sim O(1)$, re-arranging we see that

$$\Delta p \left(\frac{-1}{\gamma-1}\right) \sim \Delta \rho \left(\frac{-M_\infty^2\gamma - 1}{M_\infty^2(\gamma-1)}\right), \tag{2.18}$$

and since M_∞^2 and γ are constant, we have

$$\Delta \rho \sim \Delta p. \tag{2.19}$$

[3]Here $\sim$ implies quantities are of the same order of magnitude.

Now that we have a relation between variation in pressure and variations in velocity and density, let us consider two adjacent stream filaments in the boundary-layer. Since we expect the pressure increase to slow the fluid particles down in the boundary-layer, to conserve mass, stream filaments must be displaced to cover a wider area. Let us assume the distance between the two stream filaments is initially δ_i, which are displaced by $\Delta\delta_i$ through the interaction region as shown in Figure 2.1.

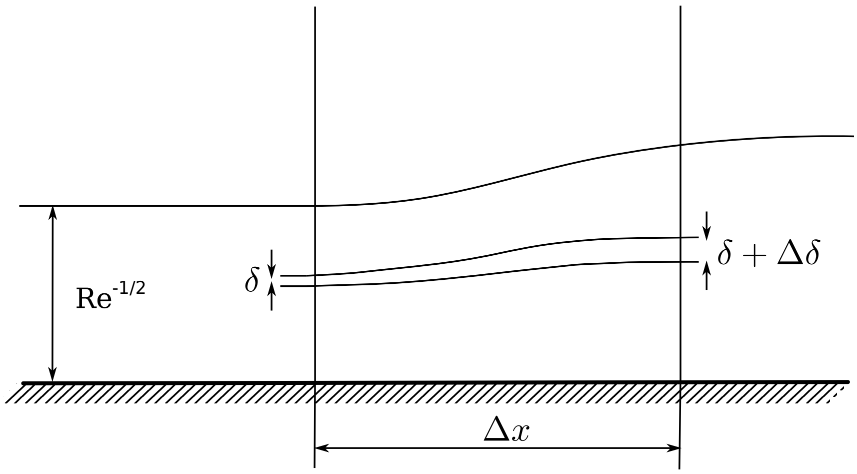

Figure 2.1*:* Viscous-inviscid interaction with thickening of stream filaments in the boundary-layer across the interaction region Δx.

By considering the i^{th} filament and the conservation of mass we see that

$$\begin{aligned}\rho_{00}U_{00}\delta_i &= (\rho_{00}+\Delta\rho)(U_{00}+\Delta u)(\delta_i+\Delta\delta_i)\\ &= \rho_{00}U_{00}\delta_i + \rho_{00}\delta_i\Delta u + \rho_{00}U_{00}\Delta\rho + \rho_{00}U_{00}\Delta\delta_i + \delta_i\Delta\rho + \\ &\quad + \rho_{00}\Delta u\Delta\delta_i + U_{00}\Delta\rho\Delta\delta_i + \Delta\rho\Delta u\Delta\delta.\end{aligned} \tag{2.20}$$

However, since the variations are very small and therefore neglecting multiples of variations, we obtain

$$\frac{\Delta\delta_i}{\delta_i} \sim \frac{\Delta u}{U_{00}} + \frac{\Delta\rho}{\rho_{00}}. \tag{2.21}$$

From equations (2.13) and (2.19), and since ρ_{00} and U_{00} are quantities of order one, we can see that the variation in the thickness of the stream filament is given by

$$\Delta\delta_i = \delta_i\Delta p. \tag{2.22}$$

Hence, the total variation in thickness of the boundary-layer due to the change in pressure is given by

$$\Delta\delta \sim \sum_i \Delta\delta_i \sim \Delta p\sum_i \delta_i \sim Re^{-1/2}\Delta p. \tag{2.23}$$

2.2.2 Near wall sublayer

One must note, close to the boundary, equation (2.9) suggests that the U_{00} tends to zero as $Y \to 0$, and therefore equation (2.12) predicts unbounded growth of the velocity variation, which is not physical. Thus, we consider a viscous sublayer close to the wall, where $\Delta u \sim U_{00}$. Hence, from (2.12) we see that

$$\Delta u U_{00} \sim \Delta u^2 \sim \frac{\Delta p}{\rho_{00}}, \tag{2.24}$$

hence, we have

$$\Delta u \sim (\Delta p)^{1/2}. \tag{2.25}$$

Thus, from the formula for U_{00} given in equation (2.9), we can conclude that

$$Y \sim (\Delta p)^{1/2}. \tag{2.26}$$

Hence, the thickness of the viscous sublayer near the wall is

$$y = Re^{-1/2} Y \sim Re^{-1/2} (\Delta p)^{1/2}. \tag{2.27}$$

Thus, for high Reynolds number the thickness of the sublayer near the wall is small. To estimate the variation in the thickness of the sublayer we turn to the conservation of mass, and since the variation of speed along the sublayer is the same as the initial speed, we deduce that the variation in thickness of the boundary-layer is comparable to the initial thickness. Therefore the variation in thickness in the sublayer is given by

$$\Delta\delta \sim Re^{-1/2} (\Delta p)^{1/2}. \tag{2.28}$$

Through the introduction of the boundary-layer, the intention is to recover viscous terms from the Navier-Stokes equations and to re-instate the no-slip condition on the boundary (the answer to d'Alembert's paradox). Therefore, we expect the sublayer to be viscous, hence it is referred to as the *viscous sublayer*. This can be shown by considering the incompressible Bernoulli equation which would apply if the flow in the sublayer was inviscid, in which case we would have

$$\frac{u^2}{2} + \frac{p^* + \Delta p}{\rho} = \frac{U_{00}^2}{2} + \frac{p^*}{\rho}, \tag{2.29}$$

where p^* represents the unperturbed pressure upstream. Re-arranging we have

$$\frac{u^2}{2} = \frac{U_{00}^2}{2} - \frac{\Delta p}{\rho}. \tag{2.30}$$

One can see that if we consider a stream line close enough to the wall, regardless of the pressure variation, the right-hand side can become negative, therefore we deduce the flow must be viscous in this sublayer.

Thus, in the sublayer, the convective terms in equation (1.9) should be balanced with the viscous terms, i.e.

$$\rho u \frac{\partial u}{\partial x} \sim \frac{1}{Re} \frac{\partial}{\partial y} \left(\mu \frac{\partial u}{\partial y} \right). \tag{2.31}$$

As before, representing the derivatives as variations we have

$$\rho_{00}U_{00}\frac{\Delta u}{\Delta x} \sim \frac{1}{Re}\frac{1}{\Delta y}\left(\mu_{00}\frac{\Delta u}{\Delta y}\right). \tag{2.32}$$

Since the density and viscosity in the sublayer, moreover in the boundary-layer, are quantities of order one and since the variation in thickness of the sublayer is comparable to its initial thickness, i.e. $y \sim \Delta y$, we have

$$\frac{U_{00}}{\Delta x} \sim \frac{1}{Re}\left(\frac{1}{y^2}\right). \tag{2.33}$$

Now, since the variation of velocity in the sublayer is comparable to the initial velocity U_{00}, let us write $u \sim \Delta u \sim U_{00}$ in the sublayer. Thus, from equations (2.25), (2.27) and (2.33), so far we have

$$u \sim (\Delta p)^{1/2}, \qquad y \sim Re^{-1/2}(\Delta p)^{1/2}, \qquad \Delta x \sim uy^2 Re. \tag{2.34}$$

2.2.3 Ackeret formula and the outer flow

To close the set of equations given in (2.34), another relationship is required which relates variation in pressure p, to variation in longitudinal distance x. In order to gain a relationship between these two quantities, let us consider the affect the pressure variation in the outer inviscid flow region has on the streamlines in the viscous sublayer.

One can see that the variation in thickness of the sublayer given in (2.28), is much larger than that of the variation in the main part of the boundary-layer given in (2.23), for $\Delta p \ll 1$. Thus, the slope angle Θ of the streamlines at the outer edge of the boundary-layer is based on the displacement of the sublayer. Since for small Θ, $\tan(\Theta) \approx \Theta$, we can approximate the slope angle as

$$\Theta \sim \frac{\Delta \delta}{\Delta x} \sim \frac{Re^{-1/2}\Delta p^{1/2}}{\Delta x}. \tag{2.35}$$

Here Θ denotes the angle at which the stream lines are displaced from their original position upstream, due to the variation in pressure.

The following formula, known as the *Ackeret formula*, was first derived by Jakob Ackeret via linearised theory when considering inviscid supersonic flow past an aerofoil. It's derivation is analogous in this case[4] , where perturbations of order $O(Re^{-1/2})$ to the uniform free are caused by the boundary-layer. In dimensional form, for supersonic flow, the equation reads

$$\hat{p} = p_\infty + \rho_\infty V_\infty^2 \frac{1}{\sqrt{M_\infty^2 - 1}}\Theta(\hat{x}). \tag{2.36}$$

This formula allows to calculate the pressure at the plate surface since the pressure does not vary across the boundary-layer, as given by equation (2.3b). Converting this to non-

[4]For a derivation of the Ackeret formula which is omitted here, the reader is referred to the book by Liepmann & Roshko (1988); see page 109.

dimensional form (for the induced pressure) and differentiating both sides, we have

$$\frac{\partial \mathbb{P}}{\partial x} = \frac{1}{\sqrt{M_\infty^2 - 1}} \frac{\partial \Theta}{\partial x}, \tag{2.37}$$

writing the derivative as variations described earlier, and since M_∞ and γ are finite constant order one quanties related to the unperturbed free stream, we have that[5]

$$\Delta p \sim \Delta \Theta. \tag{2.38}$$

However, since the streamlines along the boundary surface are initially horizontal, i.e. $\Theta = 0$, then we may write $\Delta\Theta \sim \Theta$. Hence, using equation (2.35) we finally have

$$(\Delta p)^{1/2} \sim \frac{Re^{-1/2}}{\Delta x}. \tag{2.39}$$

Hence, equation (2.39) together with (2.34) can be solved to calculate the order of magnitude of the velocity, characteristic thickness, induced pressure and characteristic width of the interaction region as given bellow, respectively.

$$u \sim Re^{-1/8}, \qquad y \sim Re^{-5/8}, \qquad \Delta p \sim Re^{-1/4}, \qquad \Delta x \sim Re^{-3/8}. \tag{2.40}$$

Before we proceed, it remains to find an estimate for the normal velocity component v, which can be obtained by considering the continuity equation (1.5). The terms in this should balance, giving

$$\frac{\partial \rho u}{\partial x} \sim \frac{\partial \rho v}{\partial y}. \tag{2.41}$$

Taking into account that the density is order one and using notation as above, we see that

$$\frac{u}{\Delta x} \sim \frac{v}{y}. \tag{2.42}$$

Hence, using (2.40) and re-arranging, we have

$$v \sim Re^{-3/8}. \tag{2.43}$$

Recall, since the initial pressure variation is caused by the presence of the shock wave in the vicinity of the interaction region, by (2.40) it is justifiable to assume, if the shockwave is weak, $p_0(x-1) \sim O(Re^{-1/4})$. This concludes the inspection analysis.

2.3 Triple-Deck Structure

Triple-deck theory (also known as asymptotic interaction theory) was first introduced simultaneously by K. Stewartson & G. Williams (1969) and Y. Nieland (1969), which was later generalised by Stewartson (1974). It presents a three-tiered structure (see Figure 2.2), in which asymptotic expansions of sought functions are constructed based on the region of interest.

[5]Here Δp denotes variation of the induced pressure $\mathbb{P}$.

Region ① is known as the viscous sublayer, region ② as the main part of the boundary-layer and region ③ represents the inviscid outer flow outside of the boundary-layer. As established from the inspection analysis, the boundary-layer interacts with the outer inviscid flow, a process known as *viscid-inviscid interaction*, and covers a longitudinal vicinity of $O(Re^{-3/8})$. The thickness of the viscous sublayer is estimated as $O(Re^{-5/8})$ and the velocity in this region is estimated as $O(Re^{-1/8})$ relative to the free stream velocity. As the motion of the fluid is much slower in the viscous sublayer, it is more susceptible to variations in pressure causing the streamlines in region ① to deform, a process known as the displacement of the boundary-layer.

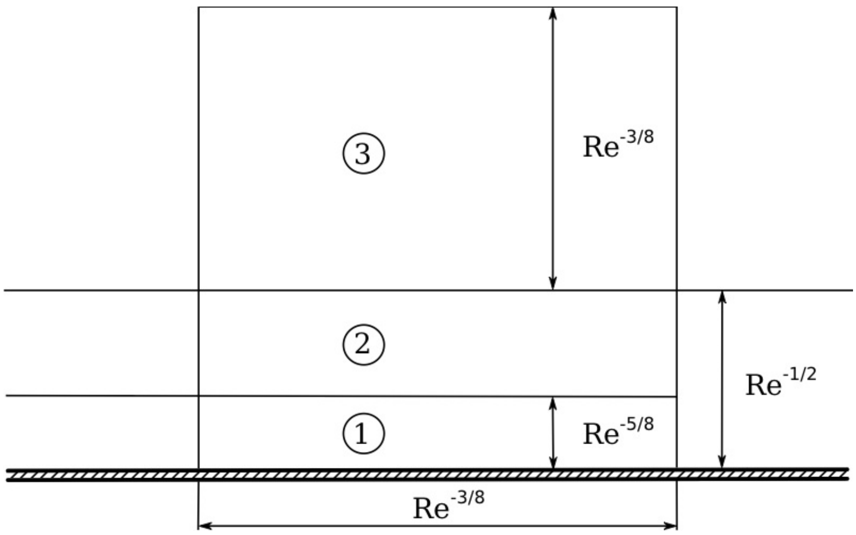

Figure 2.2*:* Three-tiered (triple-deck) structure of the interaction region.

The main part of the boundary-layer (region ②) represents the conventional boundary-layer in which the scale, as in classical boundary-layer theory, is estimated as $O(Re^{-1/2})$. The displacement effect of this part of the boundary-layer is significantly less than that of the viscous sublayer, and thus region ② simply transmits the deformation of the viscous sublayer to the outer edge of the boundary-layer. Therefore, the streamlines in region ② are parallel. Also, the velocity in this region is a quantity of order one.

Finally, we have the inviscid flow region, denoted as region ③. This tier converts the deformation in the streamlines into pressure perturbation, which is then transmitted back through the main part of the boundary-layer (region ②), to the viscous sublayer, where the streamlines deform further, eventually deflecting from the boundary surface. The free-interaction process, as described before, is self sustained and grows monotonically.

2.3.1 Viscous sublayer

We start by firstly analysing the flow in the viscous sublayer. When equations (1.3)-(1.7) were non-dimensionalised, the shock impingement, which instigates viscous-inviscid interaction, was positioned at $x = 1$. Since we are interested in the asymptotic analysis in the vicinity of this point, i.e. $|x-1| = O(Re^{-3/8})$, based on estimates (2.40) and (2.43), we begin with the following limit procedure.

$$x_* = \frac{x-1}{Re^{-3/8}} = O(1), \qquad Y_* = \frac{y}{Re^{-5/8}} = O(1), \qquad Re \to \infty. \tag{2.44}$$

The corresponding solutions to the Navier-Stokes equations may be expressed in the following asymptotic expansions.

$$\begin{aligned}
u(x,y;Re) &= Re^{-1/8}U^*(x_*,Y_*) + \dots, & \rho(x,y;Re) &= \rho^*(x_*,Y_*) + \dots,\\
v(x,y;Re) &= Re^{-3/8}V^*(x_*,Y_*) + \dots, & \mu(x,y;Re) &= \mu^*(x_*,Y_*) + \dots,\\
\mathbb{P}(x,y;Re) &= Re^{-1/4}P^*(x_*,Y_*) + \dots, & h(x,y;Re) &= h^*(x_*,Y_*) + \dots.
\end{aligned} \tag{2.45}$$

Here the enthalpy, viscosity and density remain functions of order one throughout the boundary-layer, assuming there is no extreme temperature variations of the boundary surface. So, substituting (2.45) into the Navier-Stokes equations (1.9)-(1.13) and considering the leading order terms, we obtain

$$\rho^* U^* \frac{\partial U^*}{\partial x_*} + \rho^* V^* \frac{\partial U^*}{\partial Y_*} = -\frac{\partial P^*}{\partial x_*} + \frac{\partial}{\partial Y_*}\left(\mu^* \frac{\partial U^*}{\partial Y_*}\right), \tag{2.46a}$$

$$\frac{\partial P^*}{\partial Y_*} = 0, \tag{2.46b}$$

$$\frac{\partial}{\partial x_*}(\rho^* U^*) + \frac{\partial}{\partial Y_*}(\rho^* V^*) = 0, \tag{2.46c}$$

$$\rho^* U^* \frac{\partial h^*}{\partial x^*} + \rho^* V^* \frac{\partial h^*}{\partial Y_*} = \frac{1}{Pr}\frac{\partial}{\partial Y}\left(\mu^* \frac{\partial h^*}{\partial Y_*}\right), \tag{2.46d}$$

$$h^* = \frac{1}{M_\infty^2(\gamma-1)\rho^*}. \tag{2.46e}$$

Now, from the inspection analysis we know the viscous sublayer is much thinner compared to the main part of the boundary-layer, and that the motion of the gas in this sublayer is slow. Hence, the motion in this region can be considered incompressible. To prove this point, we will start by considering the energy equation (2.46d). Since the equation is parabolic second order in Y_* and first order in x_*, it requires three boundary conditions. The first condition comes from matching the solution upstream of the interaction region (see section 2.1), i.e. as $x_* \to -\infty$. The asymptotic expansion of the enthalpy upstream is given in (2.2), which reads

$$h(x,y;Re) = h_0(x,Y) + \dots. \tag{2.47}$$

To match the solution, we re-expand (2.47) in terms of the inner variables, as given in (2.44). Re-arranging we see that

$$x - 1 = Re^{-3/8}x_*, \tag{2.48}$$

which is small. Hence we can make used of the Taylor expansion (2.8), giving

$$h(x,y;Re) = h_{00}(Y) - Re^{-3/8}x_* h_{01}(Y) + \dots. \tag{2.49}$$

Since region ①, the viscous sublayer, is much thinner than the main part of the boundary-layer, let us compare the transverse scaling of the variables. In the boundary-layer upstream we have $y = Re^{-1/2}Y$, whilst in the viscous sublayer in the interaction region we have $y = Re^{-5/8}Y_*$. Hence, we have

$$Y = Re^{-1/8}Y_*. \tag{2.50}$$

Since $Y_* = O(1)$, (2.50) implies Y is small, i.e. $Y \to 0$ as $Re \to \infty$. Therefore we can utilise (2.9), where we have

$$h(x, y; Re) = h_w + \dots . \tag{2.51}$$

Recall, h_w is a constant quantity of order one. Formula (2.51) represents the inner re-expansion of the solution upstream of the interaction region. Comparing this with the inner asymptotic expansion in region ① given in (2.45), we obtain one of the sought matching conditions given by

$$h^* \to h_w \qquad \text{as} \qquad x_* \to -\infty. \tag{2.52}$$

For simplicity, as mentioned earlier, we assume the boundary-surface is thermally isolated as given in (2.7). In region ① this can be written

$$\frac{\partial h^*}{\partial Y_*} = 0 \qquad \text{at} \qquad Y_* = 0. \tag{2.53}$$

Now, we turn to the outer edge of the viscous sublayer as $Y_* \to \infty$. We match the asymptotic solution in region ① with region ② where the flow is considered inviscid, through the agency of an intermediate region known as the overlap region. In the inviscid part of the boundary-layer (region ②) we expect the viscous terms to disappear. Thus, equation (2.46d) becomes

$$\rho^* U^* \frac{\partial h^*}{\partial x^*} + \rho^* V^* \frac{\partial h^*}{\partial Y_*} = 0. \tag{2.54}$$

Since we're considering the steady case, this states that there is no change in enthalpy following a fluid particle or along a streamline. Since the streamlines originate upstream of the interaction region where (2.52) holds, we can integrate (2.54) with (2.52) and so we conclude that

$$h^* \to h_w \qquad \text{as} \qquad Y_* \to \infty. \tag{2.55}$$

Since the wall is thermally isolated, we can prescribe a constant boundary surface temperature, i.e. $h^* = h_w$ at $Y_* = 0$, which does not vary across the viscous sublayer. Hence, we have demonstrated that the enthalpy is constant everywhere in region ①. Thus, if we turn to the equation of state (2.46e), we see that the density in region ① must also be constant. Therefore the flow in region ① is considered incompressible. Recall, in an incompressible viscous flow, the dynamic viscosity is a function of temperature alone, and since we prescribe a constant temperature which does not vary across the viscous sublayer, μ^* must also be constant. For consistency we write

$$h^* = h_w, \qquad \rho^* = \rho_w, \qquad \mu^* = \mu_w.$$

Now let us consider the momentum and continuity equations in region ①. Firstly, from the transverse momentum equation (2.46b), we see that the pressure P^* is a function of x^* alone. Hence, equations (2.46a) and (2.46c) can be written

$$\rho_w U^* \frac{\partial U^*}{\partial x_*} + \rho_w V^* \frac{\partial U^*}{\partial Y_*} = -\frac{dP^*}{dx_*} + \mu_w \frac{\partial^2 U^*}{\partial Y_*^2}, \tag{2.56a}$$

$$\frac{\partial U^*}{\partial x_*} + \frac{\partial V^*}{\partial Y_*} = 0. \tag{2.56b}$$

These equations represent the classical boundary-layer equations in the viscous sublayer and should be solved with the no-slip boundary condition

$$U^* = V^* = 0 \qquad \text{at} \qquad Y^* = 0. \tag{2.57}$$

Since the boundary-layer equations (2.56) are second order, we require another boundary condition, which again, can be formulated by matching the solution upstream of the interaction region. The asymptotic expansion of the longitudinal velocity in this region, as shown in (2.2) is given by

$$u(x, y; Re) = U_0(x, Y) + \dots. \tag{2.58}$$

As before, we re-expand (2.58) in terms of the inner variables (2.44) of region ①. Starting with the longitudinal variable as given in (2.48). Therefore, (2.58) can be represented via the Taylor expansion (2.8) to give

$$u(x, y; Re) = U_{00}(x, Y) + O(Re^{-3/8}) + \dots. \tag{2.59}$$

Considering the transverse variable as given in (2.50), we see that Y is small and hence, from (2.9) we can write

$$u(x, y; Re) = Re^{-1/8} \lambda Y_* + \dots. \tag{2.60}$$

Now, comparing the asymptotic expansion (2.60) with the asymptotic expansion in region ① from (2.45), we have to leading order, the condition

$$U^* = \lambda Y_* \qquad \text{as} \qquad x_* \to -\infty. \tag{2.61}$$

Considering the continuity equation (2.56b), a stream function ψ^*, say, can be defined such that

$$U^* = \frac{\partial \psi^*}{\partial Y_*}, \qquad V^* = -\frac{\partial \psi^*}{\partial x_*}. \tag{2.62}$$

Through the agency of the stream function, we can analyse the asymptotic behaviour of the solution to equation(2.56a) at the outer edge of the viscous sublayer, i.e. as $Y_* \to \infty$. For the stream function, we try the following "natural" form for the asymptotic expansion as the "power function" given by[6]

$$\psi^*(x_*, Y_*) = A_0(x_*) Y_*^{\alpha} + \dots \qquad \text{as} \qquad Y_* \to \infty. \tag{2.63}$$

The parameter α and function $A_0(x_*)$ are to be found via the momentum equation (2.56a).

[6]This form of asymptotic expansion has been employed previously, for example in the paper by K. Stewartson (1969).

We proceed by first substituting the stream function into (2.62), from which we obtain

$$U^* = \alpha A_0 Y_*^{\alpha-1} + \dots, \tag{2.64a}$$

$$V^* = -\frac{dA_0}{dx_*} Y_*^{\alpha} + \dots. \tag{2.64b}$$

Thus the convective and viscous terms in the momentum equation (2.56a) are given by

$$\rho_w U^* \frac{\partial U^*}{\partial x_*} = \rho_w \alpha^2 A_0 \frac{dA_0}{dx_*} Y_*^{2\alpha-2} + \dots, \tag{2.65a}$$

$$\rho_w V^* \frac{\partial U^*}{\partial Y_*} = -\rho_w \alpha(\alpha-1) A_0 \frac{dA_0}{dx_*} Y_*^{2\alpha-2} + \dots, \tag{2.65b}$$

$$\mu_w \frac{\partial^2 U^*}{\partial Y_*^2} = \mu_w \alpha(\alpha-1)(\alpha-2) A_0 Y_*^{\alpha-3} + \dots. \tag{2.65c}$$

Now, as $Y_* \to \infty$, the pressure gradient remains finite, and so, if we substitute (2.64) and (2.65) into the momentum equation (2.56a), the terms which will dominate for $\alpha > 1$ are the terms of $O(Y^{2\alpha-2})$, reducing (2.56a) to

$$A_0 \frac{dA_0}{dx_*} = 0.$$

The initial condition for this equation can be obtained by substituing (2.64a) into (2.61), producing

$$A_0(-\infty) = \begin{cases} \lambda/\alpha & \text{if} \quad \alpha = 2 \\ 0 & \text{if} \quad \alpha \neq 2 \end{cases}.$$

So there exists a non-trivial solution for A_0 if $\alpha = 2$, for which we can write

$$\psi^*(x_*, Y_*) = \frac{\lambda}{2} Y_*^2 + A_1(x_*) Y_*^{\bar{\alpha}} + \dots \qquad \text{as} \qquad Y_* \to \infty, \tag{2.66}$$

where $A_1(x_*) Y_*^{\bar{\alpha}}$ represents the second term in the asymptotic expansions of ψ^*. To ensure that this term is smaller than the first, we will impose $\bar{\alpha} < 2$. Substituing (2.66) into (2.62) we have

$$U^* = \lambda Y_* + \bar{\alpha} A_1 Y_*^{\bar{\alpha}-1} + \dots, \tag{2.67a}$$

$$V^* = -\frac{dA_1}{dx_*} Y_*^{\bar{\alpha}} + \dots. \tag{2.67b}$$

So, once again we can compute the convective and viscous terms from (2.56a), which can be written as

$$\rho_w U^* \frac{\partial U^*}{\partial x_*} = \rho_w \bar{\alpha} \frac{dA_1}{dx_*} Y_*^{\bar{\alpha}} + \dots, \tag{2.68a}$$

$$\rho_w V^* \frac{\partial U^*}{\partial Y_*} = -\rho_w \lambda \frac{dA_1}{dx_*} Y_*^{\bar{\alpha}} + \dots, \tag{2.68b}$$

$$\mu_w \frac{\partial^2 U^*}{\partial Y_*^2} = \mu_w \bar{\alpha}(\bar{\alpha}-1)(\bar{\alpha}-2) A_1 Y_*^{\alpha-3} + \dots. \tag{2.68c}$$

Now, following the procedure as before, the convective terms that dominate the momentum equation (2.56a) if $\bar{\alpha} > 0$ are of $O(Y_*^{\bar{\alpha}})$. Considering these terms reduces (2.56a) to

$$\frac{dA_1}{dx_*} = 0. \tag{2.69}$$

Since the condition (2.61) only has one term which matches the leading order term of ψ^*, we conclude that

$$A_1(-\infty) = 0 \qquad \text{if} \qquad \bar{\alpha} \neq 1.$$

However, if $\bar{\alpha} = 1$, there exists a non-trivial solution for A_1. The function $A_1(x_*)$ remains arbitrary in the asymptotic expansion of the stream function, which can be determined later. Thus, we finally have

$$\psi^*(x_*, Y_*) = \frac{\lambda}{2}Y_*^2 + A_1(x_*)Y_* + \dots \qquad \text{as} \qquad Y_* \to \infty. \tag{2.70}$$

Before we proceed, we consider the streamline slope angle produced by the deflection of the streamlines in the viscous sublayer. We can calculate the slope angle θ by considering the velocity components in the viscous sublayer as

$$\Theta = \tan^{-1}\left(\frac{v}{u}\right).$$

Substituting (2.70) into (2.62), we see that at the outer edge of the viscous sublayer we have

$$U^* = \lambda Y_* + A_1(x_*) + \dots, \qquad V^* = -\frac{dA_1}{dx_*}Y_* + \dots. \tag{2.71}$$

Now, in the viscous sublayer (region ①) the asymptotic expansion of the velocity components are

$$u = Re^{-1/8}U^*(x_*, Y_*) + \dots, \qquad v = Re^{-3/8}V^*(x_*, Y_*) + \dots,$$

therefore

$$u = Re^{-1/8}\lambda Y_* + Re^{-1/8}A_1(x_*) + \dots, \qquad v = -Re^{-3/8}\frac{dA_1}{dx_*}Y_* + \dots. \tag{2.72}$$

Hence, we can conclude that the streamline slope angle at the outer edge of the viscous sublayer is given by

$$\Theta = \tan^{-1}\left[\frac{V^*(x_*, \infty)}{U^*(x_*, \infty)}\right] \approx Re^{-1/4}\frac{V^*(x_*, \infty)}{U^*(x_*, \infty)} + \dots \approx -Re^{-1/4}\frac{1}{\lambda}\frac{dA_1}{dx_*} + \dots.$$

Henceforth, due to the relation to θ, $A_1(x_*)$ is known as the *displacement function.*

2.3.2 Main part of the boundary-layer

Now let us turn to region ② of the triple-deck model. This tier, along with the viscous sublayer form what is conventionally known as the boundary-layer. The vertical extent of this region is given by its thickness which is estimated as $y = O(Re^{-1/2})$ as given in (2.1), whilst the longitudinal extent considered is the vicinity of the interaction region, which as before is estimated as $|x-1| = O(Re^{-3/8})$. Hence, the asymptotic analysis in region ② is based on the limit procedure

$$x_* = \frac{x-1}{Re^{-3/8}} = O(1), \qquad Y = \frac{y}{Re^{-1/2}} = O(1), \qquad Re \to \infty. \tag{2.73}$$

To calculate the asymptotic expansions of the solutions to the Navier-Stoes equations in region ②, we consider the asymptotic expansion in the overlap region which lies between regions ① and ②. Firstly, we consider the solution of the velocity components at the outer edge of region ①, which are given in (2.72). To gain the solution at the bottom of region ②, we simply re-expand these solutions in terms of the variables (2.73). Since variable x_* remains the same in both regions, we need only compare the "y" variables in (2.44) and (2.73), which gives $Y_* = Re^{1/8}Y$. Hence, re-expanding the velocity components in terms of these variables we have

$$u(x_*, Y; Re) = \lambda Y + Re^{-1/8} A_1(x_*) + \dots, \tag{2.74a}$$

$$v(x_*, Y; Re) = -Re^{-1/4} \frac{dA_1}{dx_*} Y + \dots. \tag{2.74b}$$

Since we are considering the bottom of region ②, i.e. as $Y \to 0$, we see the first term of u in (2.74) coincides with the asymptotic expansion in (2.9), where

$$U_{00}(Y) = \lambda Y + \dots \qquad \text{as} \qquad Y \to 0. \tag{2.75}$$

So, the asymptotic expansions of the velocity components in region ② can be written as

$$\begin{aligned} u(x,Y; Re) &= U_{00}(Y) + Re^{-1/8} \breve{U}_1(x_*, Y) + \dots, \\ v(x, Y; Re) &= Re^{-1/4} \breve{V}_1(x_*, Y) + \dots. \end{aligned} \tag{2.76}$$

To match these solutions with the outer solution of region ①, the solution in region ② must satisfy the matching condition

$$\breve{U}_1 = A_1(x_*) + \dots, \qquad \breve{V}_1 = -\frac{dA_1}{dx_*} Y + \dots \qquad \text{as} \qquad Y \to 0. \tag{2.77}$$

Now, since the pressure does not change across the viscous sublayer, i.e. region ①, due to (2.46b) , the pressure perturbations in region ② should be of the same order as in region ①. Hence, in terms of the variables in region ②, we expect pressure perturbations to be $O(Re^{-1/4})$, therefore we write

$$\mathbb{P}(x, y; Re) = Re^{-1/4} \breve{P}(x_*, Y) \quad + \dots. \tag{2.78}$$

In light of the expansion for the longlitudinal velocity u in region ②, and referring to (2.45), we see that the sought density, viscosity and enthalpy functions are described by the following asymptotic expansions, in terms of the variables in (2.73).

$$\begin{aligned} \rho(x, y; Re) &= \rho_{00}(Y) + Re^{-1/8} \breve{\rho}_1(x_*, Y) + \dots, \\ \mu(x, y; Re) &= \mu_{00}(Y) + Re^{-1/8} \breve{\mu}_1(x_*, Y) + \dots, \\ h(x, y; Re) &= h_{00}(Y) + Re^{-1/8} \breve{h}_1(x_*, Y) + \dots. \end{aligned} \tag{2.79}$$

Substituting the asymptotic expansions (2.77), (2.78) and (2.79) into the Navier-Stokes equations (1.9)-(1.13), and considering leading order terms (order $O(Re^{1/4})$) which dominate, the equations (1.9)-(1.12) reduce to

$$U_{00}\frac{\partial \breve{U}_1}{\partial x_*} + \breve{V}_1\frac{dU_{00}}{dY} = 0, \tag{2.80a}$$

$$\frac{\partial \breve{P}_1}{\partial Y} = 0, \tag{2.80b}$$

$$\rho_{00}\frac{\partial \breve{U}_1}{\partial x_*} + U_{00}\frac{\partial \breve{\rho}_1}{\partial x_*} + \rho_{00}\frac{\partial \breve{V}_1}{\partial Y} + \breve{V}_1\frac{d\rho_{00}}{dY} = 0, \tag{2.80c}$$

$$U_{00}\frac{\partial \breve{h}_1}{\partial x_*} + \breve{V}_1\frac{dh_{00}}{dY} = 0. \tag{2.80d}$$

For the state equation (1.13), we use the approximation

$$\frac{1}{\rho} = \frac{1}{\rho_{00} + Re^{-1/8}\breve{\rho}_1} = \frac{1}{\rho_{00}}\left(1 - Re^{-1/8}\frac{\breve{\rho}_1}{\rho_{00}} + \dots\right).$$

Hence, to $O(1)$ we have

$$h_{00} = \frac{1}{M_\infty^2(\gamma-1)}\frac{1}{\rho_{00}}, \tag{2.81}$$

and to $O(Re^{-1/8})$ we have

$$\breve{h}_1 = -\frac{1}{M_\infty^2(\gamma-1)}\frac{\breve{\rho}_1}{\rho_{00}^2}. \tag{2.82}$$

Equations (2.80)-(2.82) can be solved through the following elimination process. First let us eliminate h_{00} and $\breve{h}_1$ by substituting (2.81) and (2.82) into the energy equation (2.80d), which yields

$$U_{00}\frac{\partial \breve{\rho}_1}{\partial x_*} + \breve{V}_1\frac{d\rho_{00}}{dY} = 0. \tag{2.83}$$

Hence the continuity equation (2.80c) can be written

$$\frac{\partial \breve{U}_1}{\partial x_*} + \frac{\partial \breve{V}_1}{\partial Y} = 0. \tag{2.84}$$

Now, eliminating $\breve{U}_1$ terms from the momentum equation (2.80a) and equation (2.84) we have

$$-U_{00}\frac{\partial \breve{V}_1}{\partial Y} + \breve{V}_1\frac{dU_{00}}{dY} = 0. \tag{2.85}$$

Dividing (2.85) by U_{00}^2 we have

$$-\frac{1}{U_{00}}\frac{\partial \breve{V}_1}{\partial Y} + \frac{1}{U_{00}^2}\breve{V}_1\frac{dU_{00}}{dY} = \frac{\partial}{\partial Y}\left[\frac{\breve{V}_1}{U_{00}}\right] = 0. \tag{2.86}$$

Therefore $\breve{V}_1/U_{00}$ is a function of x_* alone, i.e. it remains the same vertically across region ②. Considering $\breve{V}_1$ and U_{00} at the bottom of region ②, which are given in formulae (2.75) and (2.77), we see that

$$\frac{\breve{V}_1}{U_{00}} = -\frac{1}{\lambda}\frac{dA_1}{dx_*}. \tag{2.87}$$

Thus, if we consider the slope displacement angle of the streamlines in region ②, using the expansion for velocity components given in (2.76) , we have, to leading order

$$\Theta = \tan^{-1}\left(\frac{v}{u}\right) = \frac{Re^{-1/4}\breve{V}_1}{U_{00} + Re^{-1/4}\breve{U}_1} + \cdots = Re^{-1/4}\frac{\breve{V}_1}{U_{00}} + \cdots = -Re^{-1/4}\frac{1}{\lambda}\frac{dA_1}{dx_*} + \cdots. \tag{2.88}$$

Hence, the slope angle Θ remains unchanged through the main part of the boundary-layer. This confirms that the main part of the boundary-layer does not contribute to the displacement of the streamlines. It simply transports the deformation from the viscous sublayer to bottom of the the outer flow, region ③ in the triple-deck structure (see Figure 2.2).

2.3.3 Interaction law

Finally, we turn to the lower part of region ③, where the pressure variations initially originate due the existence of the weak shock wave and we note $p_0(x_*) \sim O(Re^{-1/4})$. Since the variations in thickness of the boundary-layer translate to variations in pressure in the inviscid outer flow, we turn to the Ackeret formula in it's dimensionless form, given in (2.37). From equations (2.46b) and (2.80b), we see that the pressure does not change across the entire boundary-layer spanning regions ① and ② (it is independent of y), hence the imposed pressure perturbation in region ① is given by

$$P^* = \frac{1}{\sqrt{M_\infty^2 - 1}}\Theta + p_0. \tag{2.89}$$

Since the streamline slope angle Θ is known at the outer edge of region ②, given by (2.88), we can finally write

$$P^*(x_*) = -\frac{1}{\sqrt{M_\infty^2 - 1}}\frac{1}{\lambda}\frac{dA_1}{dx_*} + p_0(x_*). \tag{2.90}$$

Where p_0 is defined in equation (1.15). Equation (2.90) provides a relationship between the displacement function $A_1(x_*)$, and the induced pressure at the bottom of region ③ - the inviscid tier. For this reason, (2.90) is known as the *interaction law.*

2.4 Canonical representation

Let us summarise what we have gained from the asymptotic analysis of the interaction problem. Starting with the viscous sublayer, we see that the "classical" boundary-layer equations (2.56) describe the flow, which are to be solved with boundary condition (2.57), and the "initial" condition (2.61). However, this problem differs from the classical boundary-layer equations as formulated by Prandtl, because the pressure along the boundary surface is unknown beforehand. Instead, the pressure is given by the interaction law (2.90). Finally, the function $A_1(x_*)$, which is related to the pressure in the interaction law, may be found with the agency of the first of equations in (2.71).

To present these equations in their canonical form, we consider the following affine transformation.

$$x_* = \frac{\mu_w^{-1/4}\rho_w^{-1/2}}{\lambda^{5/4}\beta^{3/4}}\bar{X}, \qquad A_1 = \frac{\mu_w^{1/4}\rho_w^{-1/2}}{\lambda^{-1/4}\beta^{1/4}}\bar{A}, \qquad V^* = \frac{\mu_w^{3/4}\rho_w^{-1/2}}{\lambda^{-3/4}\beta^{-1/4}}\bar{V},$$

$$Y_* = \frac{\mu_w^{1/4}\rho_w^{-1/2}}{\lambda^{3/4}\beta^{1/4}}\bar{Y}, \qquad U^* = \frac{\mu_w^{1/4}\rho_w^{-1/2}}{\lambda^{-1/4}\beta^{1/4}}\bar{U}, \qquad P^* = \frac{\mu_w^{1/2}\rho_w^{-1/2}}{\lambda^{-1/2}\beta^{1/2}}\bar{P},$$

$$p_0 = \frac{\mu_w^{1/2}\rho_w^{-1/2}}{\lambda^{-1/2}\beta^{1/2}}\bar{p}_0.$$

In the above $\beta = \sqrt{M_\infty^2 - 1}$. This allows to present the equations of the interaction problem as

$$\bar{U}\frac{\partial \bar{U}}{\partial \bar{X}} + \bar{V}\frac{\partial \bar{U}}{\partial \bar{Y}} = -\frac{d\bar{P}}{d\bar{X}} + \frac{\partial^2 \bar{U}}{\partial \bar{Y}^2}, \tag{2.91a}$$

$$\frac{\partial \bar{U}}{\partial \bar{X}} + \frac{\partial \bar{V}}{\partial \bar{Y}} = 0, \tag{2.91b}$$

$$\bar{P} = -\frac{d\bar{A}}{d\bar{X}} + \bar{p}_0, \tag{2.91c}$$

coupled with the following conditions (as described above)

$$\bar{U} = \bar{V} = 0 \qquad \text{at} \quad \bar{Y} = 0, \tag{2.92a}$$

$$\bar{U} = \bar{Y} + \bar{A}(\bar{X}) \qquad \text{as} \quad \bar{Y} \to \infty, \tag{2.92b}$$

$$\bar{U} = \bar{Y} + \dots \qquad \text{as} \quad \bar{X} \to -\infty. \tag{2.92c}$$

Note, $\bar{P}$ is a function of $\bar{X}$ alone as it does not vary across the boundary-layer, and in terms of the variable $\bar{X}$, $\bar{p}_0(\bar{X}) = \alpha_0 H(\bar{X})$, where $H(\bar{X})$ is the *Heaviside step function* defined as

$$H(\bar{X}) = \begin{cases} 1 & \text{for all } \bar{X} > 0 \\ 0 & \text{for all } \bar{X} < 0 \end{cases}.$$

This concludes the formulation of the interaction problem for an oblique shock wave impinging on a laminar boundary-layer (see Figure 1.2).

3 Varying Plate Speeds

Much of the work presented to date consider the situation in which the plate is at rest, where the upstream influence was first discovered. In this section we will extend the interaction problem to consider situations in which the boundary or plate moves with speed V_w, say. Due to the no-slip condition, to accommodate for the moving plate, boundary condition (2.92) becomes

$$\bar{U} = V_w, \quad \bar{V} = 0 \qquad \text{at} \quad \bar{Y} = 0, \tag{3.1a}$$
$$\bar{U} = \bar{Y} + \bar{A}(\bar{X}) \qquad \text{as} \quad \bar{Y} \to \infty, \tag{3.1b}$$
$$\bar{U} = \bar{Y} + \ldots \qquad \text{as} \quad \bar{X} \to -\infty. \tag{3.1c}$$

Before we continue, we consider the following theorem by S. Kaplun.

3.1 Kaplun's Extension Theorem

The asymptotic expansions of the Navier-Stokes equations presented in the previous chapter were constructed on the limit $Re \to \infty$ and was intended for the region of interaction. However, the expansions of the solution are valid in a wider region, a result of Kaplun's Extension Theorem. Since we now vary the speed of the plate, we are interested in the affect of moving plate on the solution in the boundary-layer, and to do so, we can utilise the formulation (2.91) and (2.92) due to the following theorem.[7]

Theorem. *Let M and N be two order classes with $M \leq N$ and $f(x;\epsilon)$ an approximation to $u(x;\epsilon)$ valid to order $\xi(\epsilon)$ in the order domain $[M, N]$. Then there exist order classes $M_e < M$ and $N_e > N$ such that $f(x;\epsilon)$ is an approximation to $u(x;\epsilon)$ valid to order $\xi(\epsilon)$ in the extended order domain $[M_e, N_e]$. Here x represents the co-ordinate, scalar or vector, and ϵ is a small parameter.*

This theorem is required in what follows as we are particularly interested in the upstream influence in the boundary-layer, a result of the shock wave/boundary-layer interaction. Referring to the theorem above, it is the extension of the lower bound M_e which will allow us to investigate the solution upstream, i.e. when $\bar{X} < 0$. Note, here we consider the solution upstream of the interaction region as the "outer" solution.

3.2 Linearising the governing equations

In order to study the upstream influence in the boundary-layer, the governing equations shall be linearised. First let us consider the boundary value problem (2.91) with (2.92), which admits the following solution

$$\bar{U} = \bar{Y}, \quad \bar{V} = 0, \quad \bar{P} = 0, \quad \bar{A} = 0. \tag{3.2}$$

[7] No proof of the theorem is given here, however an interested reader is referred to the book by P. Lagerstrom (1980); see page 27.

Now, with the boundary conditions (3.1), assuming the boundary/flat plate is moving, i.e.

$$\bar{U} = V_w \quad at \quad \bar{Y} = 0,$$

the solution admitted by (2.91) with (3.1) becomes

$$\bar{U} = \bar{Y} + V_w, \quad \bar{V} = 0, \quad \bar{P} = 0, \quad \bar{A} = 0. \tag{3.3}$$

Now, assuming the shock wave which impinges on the boundary-layer is a weak shock, to study the upstream influence, the basic solution (3.3) is superimposed by a perturbation. We will also assume that the perturbations are weak, i.e. of small amplitude $\epsilon \ll 1$. So we write the solution as[8]

$$\begin{gathered}\bar{U} = \bar{Y} + V_w + \epsilon u'(\bar{X}, \bar{Y}), \quad \bar{V} = \epsilon v'(\bar{X}, \bar{Y}), \quad \bar{P} = \epsilon p'(\bar{X}), \\ \bar{A} = \epsilon A'(\bar{X}), \quad \bar{p}_0 = \epsilon p_0'(\bar{X}).\end{gathered} \tag{3.4}$$

Substituting (3.4) into the governing equations (2.91) we obtain

$$\begin{aligned}(\bar{Y} + V_w + \epsilon u')\frac{\partial}{\partial \bar{X}}(\bar{Y} + V_w + \epsilon u') + \epsilon v'\frac{\partial}{\partial \bar{Y}}(\bar{Y} + V_w + \epsilon u') = \\ = -\frac{d}{d\bar{X}}(\epsilon p') + \frac{\partial^2}{\partial \bar{Y}^2}(\bar{Y} + V_w + \epsilon u'),\end{aligned} \tag{3.5a}$$

$$\frac{\partial}{\partial \bar{X}}(\bar{Y} + V_w + \epsilon u') + \frac{\partial}{\partial \bar{Y}}(\epsilon v') = 0, \tag{3.5b}$$

$$\epsilon p' = -\frac{d}{d\bar{X}}(\epsilon A') + \epsilon p_0'(\bar{X}). \tag{3.5c}$$

Since the perturbations are weak, disregarding terms of order ϵ^2 and higher, we obtain the following linearised equations.

$$(\bar{Y} + V_w)\frac{\partial u'}{\partial \bar{X}} + v' = -\frac{dp'}{d\bar{X}} + \frac{\partial^2 u'}{\partial \bar{Y}^2}, \tag{3.6a}$$

$$\frac{\partial u'}{\partial \bar{X}} + \frac{\partial v'}{\partial \bar{Y}} = 0, \tag{3.6b}$$

$$p' = -\frac{dA'}{d\bar{X}} + \alpha_0 H(\bar{X}). \tag{3.6c}$$

3.2.1 Solving the linearised equations

Before we attempt to solve the linearised equations, let us present the corresponding boundary condition to (3.6), which are given by substituting (3.4) into (3.1). We have

$$u' = v' = 0 \qquad \text{at} \quad \bar{Y} = 0, \tag{3.7a}$$

$$u' = A'(\bar{X}) \qquad \text{as} \quad \bar{Y} \to \infty, \tag{3.7b}$$

$$u' = 0 \qquad \text{as} \quad \bar{X} \to -\infty. \tag{3.7c}$$

[8] Note, here $'$ (dash) distinguishes perturbed functions.

Now, eliminating p' between (3.6a) and (3.6c), we obtain the following equations

$$(\bar{Y}+V_w)\frac{\partial u'}{\partial \bar{X}}+v'=\frac{d^2A'}{d\bar{X}^2}-\alpha_0\delta(\bar{X})+\frac{\partial^2 u'}{\partial \bar{Y}^2}, \tag{3.8a}$$

$$\frac{\partial u'}{\partial \bar{X}}+\frac{\partial v'}{\partial \bar{Y}}=0. \tag{3.8b}$$

Note that the derivative of the Heaviside function is the Dirac delta function, i.e. $dH/d\bar{X}=\delta(\bar{X})$.

One would like to construct the solution to the boundary value problem in which the behaviour of the functions u', v' and p' upstream of the shock impingement may be found. The boundary value problem can be solved using the method of Fourier Transform in $\bar{X}$. Recall, the Fourier transform $\tilde{u}(\bar{X},\bar{Y})$ of a function $u'(\bar{X},\bar{Y})$ is calculated via the integral

$$\tilde{u}(k,\bar{X})=\mathcal{F}[u'](k)=\int_{-\infty}^{\infty}u'(\bar{X},\bar{Y})e^{-ik\bar{X}}d\bar{X}, \tag{3.9}$$

with known $\tilde{u}(\bar{X},\bar{Y})$, the original function can be restored using in inverse Fourier transform as

$$u'(\bar{X},\bar{Y})=\frac{1}{2\pi}\int_{-\infty}^{\infty}\tilde{u}(k,\bar{Y})e^{ik\bar{X}}dk. \tag{3.10}$$

Thus, it follows from (3.10), taking the Fourier transform of (3.8) we have

$$(\bar{Y}+V_w)ik\tilde{u}+\tilde{v}=-k^2\tilde{A}-\alpha_0+\frac{d^2\tilde{u}}{d\bar{Y}^2}, \tag{3.11a}$$

$$ik\tilde{u}+\frac{d\tilde{v}}{d\bar{Y}}=0. \tag{3.11b}$$

Note that the Fourier transform of the Dirac Delta function is given by $\mathcal{F}[\delta(\bar{X})](k)=1$. Now, differentiating equation (3.11a) with respect to $\bar{Y}$ yields

$$ik\tilde{u}+(\bar{Y}+V_w)ik\frac{d\tilde{u}}{d\bar{Y}}+\frac{d\tilde{v}}{d\bar{Y}}=\frac{d^3\tilde{u}}{d\bar{Y}^3}. \tag{3.12}$$

Eliminating $d\tilde{v}/d\bar{Y}$ between (3.11b) and (3.12), we have

$$(\bar{Y}+V_w)ik\frac{d\tilde{u}}{d\bar{Y}}=\frac{d^3\tilde{u}}{d\bar{Y}^3}. \tag{3.13}$$

Now that we have a differential equation for $\tilde{u}(\bar{Y})$ alone, let us make the following change of variable

$$z=\theta(\bar{Y}+V_w), \tag{3.14}$$

so that we have

$$\theta^3\frac{d^3\tilde{u}}{dz^3}-ikz\frac{d\tilde{u}}{dz}=0. \tag{3.15}$$

Hence, putting $\theta^3=ik$, we obtain the *Airy equation* for $d\tilde{u}/dz$, given below

$$\frac{d^3\tilde{u}}{dz^3}-z\frac{d\tilde{u}}{dz}=0. \tag{3.16}$$

Equation (3.16) is a third order differential equation in z, and recall $z \sim Y$, hence we require three boundary conditions for $\tilde{u}$. First, recall the boundary conditions from the linearised form of the boundary-layer equation, given in (3.7). From this, we can deduce two of the three boundary conditions required for the perturbation $\tilde{u}$ with respect to $\bar{Y}$, given below.

$$\tilde{u} = 0 \qquad \text{at} \quad \bar{Y} = 0, \tag{3.17a}$$

$$\tilde{u} = \tilde{A}(k) \qquad \text{as} \quad \bar{Y} \to \infty. \tag{3.17b}$$

For the third boundary condition we consider the momentum equation (3.11a) on the boundary i.e. the flat plate, and since $\tilde{u} = \tilde{v} = 0$ at $\bar{Y} = 0$, we obtain

$$\frac{d^2\tilde{u}}{d\bar{Y}^2} = k^2\tilde{A} + \alpha_0 \qquad \text{at} \quad \bar{Y} = 0. \tag{3.17c}$$

The general solution to equation (3.16) is given in terms of the Airy functions as

$$\frac{d\tilde{u}}{d\bar{z}} = C_1\text{Ai}(z) + C_2\text{Bi}(z), \tag{3.18}$$

where Ai and Bi are linearly independent. However, the asymptotic series representation of Bi for large $|z|$ is given by[9]

$$\text{Bi}(z) \sim \frac{1}{\sqrt{\pi}} z^{-1/4} e^{\zeta} + \dots \qquad \text{as} \qquad |z| \to \infty, \quad (|\arg(z)| < \frac{\pi}{3}). \tag{3.19}$$

Here, ζ is given by

$$\zeta = \frac{2}{3} z^{3/2}. \tag{3.20}$$

Recall, $z = \theta(\bar{Y} + V_w)$ and $\theta = (ik)^{1/3}$. Note that θ is a "three-valued" function of k (so too is z) and hence, Bi (or Ai) may be exponentially increasing or decreasing for different values of k in the k-plane. Thus, to satisfy boundary condition (3.17b), either C_1 or C_2 is required to be zero for different values of k. To keep our analysis simple, we will fix $C_2 = 0$ by taking the branch cut in the k-plane as shown in Figure 3.1(a) below.

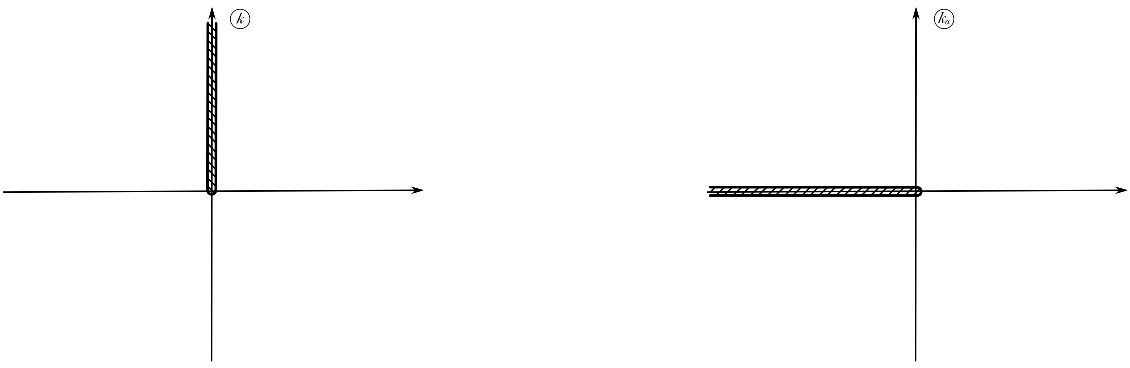

(a) Branch cut in the k-plane. (b) Branch cut in the k_α-plane.

Figure 3.1: Corresponding branch cuts in k and k_α planes, used to simplify analysis.

[9]Abramowitz & Stegun (1965); see page 449.

If we put

$$k_\alpha = ik = e^{i\frac{\pi}{2}}k = |k|e^{i(\phi+\frac{\pi}{2})},$$

where $\phi = \arg(k)$, then the branch cut simply goes through a rotation of $\pi/2$ as shown in Figure 3.1(b) above, and we have $z = k_\alpha^{1/3}(\bar{Y} + V_w)$. Hence, as $\bar{Y} \to \infty$ we write $z^{3/2} \sim k_\alpha^{1/2}\bar{Y}$. This essentially translates to a conformal mapping which limits the extent of z as shown in Figure 3.2 below.

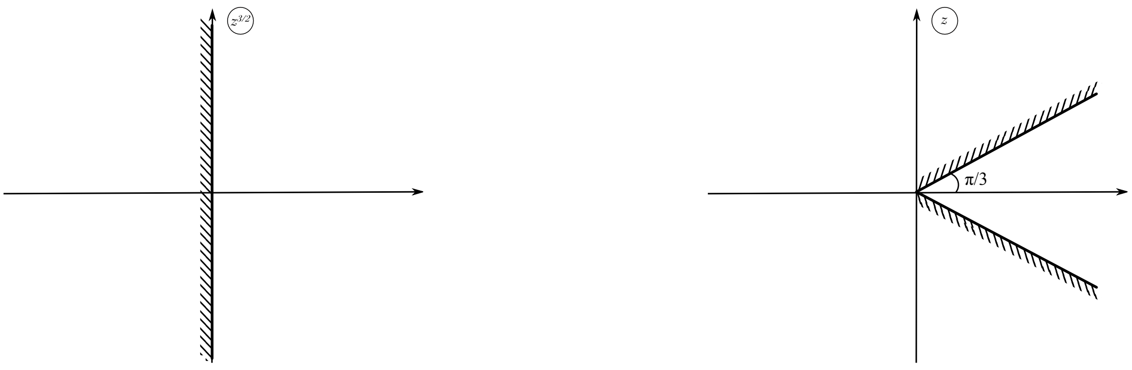

(a) The $z^{3/2}$-plane. (b) The z-plane.

Figure 3.2*:* How the branch cut in the k-plane relates to variable z.

Since $z \sim \bar{Y}$, and considering the above in which z is made single valued through the appropriate branch cut, Bi grows exponentially at the outer edge of the boundary-layer, i.e. as $\bar{Y} \to \infty$. Hence, in view of boundary condition (3.17b) we set $C_2 = 0$. Thus, we have

$$\frac{d\tilde{u}}{dz} = C_1 \mathrm{Ai}(z). \tag{3.21}$$

Here the airy function in the complex plane is defined as[10]

$$\mathrm{Ai}(z) = \frac{1}{2\pi i}\int_{-i\infty}^{i\infty} e^{zs-\frac{s^3}{3}}\,ds.$$

Now, applying boundary condition (3.17c), we need to differentiate equation (3.21), we see that[11]

$$\left.\frac{d^2\tilde{u}}{d\bar{Y}^2}\right|_{\bar{Y}=0} = \theta^2 \left.\frac{d^2\tilde{u}}{dz^2}\right|_{z=\theta V_w} = \theta^2 C_1 \mathrm{Ai}'(\theta V_w). \tag{3.22}$$

Thus, from (3.17c) we have

$$\theta^2 C_1 \mathrm{Ai}'(\theta V_w) = k^2\tilde{A} + \alpha_0, \tag{3.23}$$

hence we can write C_1 in terms of $\tilde{A}$ as

$$C_1 = \frac{k^2\tilde{A} + \alpha_0}{\theta^2 \mathrm{Ai}'(\theta V_w)}. \tag{3.24}$$

Now, in order to apply boundary condition (3.17b), we need to integrate (3.21) in order

[10]Valleé & Soares, (2004); see page 6.

[11]Note, in what follows, regarding the Airy function, prime denotes the derivative with respect to z.

to get an expression for $\tilde{u}$. Thus, we see that

$$\tilde{u} = C_1 \int_0^z \mathrm{Ai}(s)ds + C_3. \tag{3.25}$$

Applying boundary condition (3.17a) we can find C_3 as

$$C_3 = -C_1 \int_0^{\theta V_w} \mathrm{Ai}(s)ds, \tag{3.26}$$

hence

$$\tilde{u} = C_1 \left[\int_0^z \mathrm{Ai}(s)ds - \int_0^{\theta V_w} \mathrm{Ai}(s)ds \right] = C_1 \int_{\theta V_w}^z \mathrm{Ai}(s)ds. \tag{3.27}$$

Finally, applying boundary condition (3.17b) we have

$$C_1 \int_{\theta V_w}^{\infty} \mathrm{Ai}(s)ds = \tilde{A}. \tag{3.28}$$

Now, eliminating C_1 between (3.24) and (3.28) we can find the function $\tilde{A}(\bar{X})$, so we see that

$$\tilde{A} = \frac{\alpha_0 \int_{\theta V_w}^{\infty} \mathrm{Ai}(s)ds}{\theta^2 \mathrm{Ai}'(\theta V_w) - k^2 \int_{\theta V_w}^{\infty} \mathrm{Ai}(s)ds}. \tag{3.29}$$

To understand the characteristics of the flow upstream in the boundary-layer, it suffices to calculate the pressure distribution p'. So, let us consider the interaction law given in equation (3.6c). Taking the Fourier transform of this equations yields[12]

$$\tilde{p} = -ik\tilde{A} + \mathcal{F}[\alpha_0 H(\bar{X})](k). \tag{3.30}$$

Substituting for $\tilde{A}$ from equation (3.29), we have the pressure in the Fourier space at the outer edge of the viscous sublayer given by

$$\tilde{p} = -i\alpha_0 \frac{k \int_{\theta V_w}^{\infty} \mathrm{Ai}(s)s}{\theta^2 \mathrm{Ai}'(\theta V_w) - k^2 \int_{\theta V_w}^{\infty} \mathrm{Ai}(s)ds} + \mathcal{F}[\alpha_0 H(\bar{X})](k). \tag{3.31}$$

To recover the pressure perturbation $p'(\bar{X})$ we require the inverse Fourier transform of the function $\tilde{p}$. Recall

$$p'(\bar{X}) = \frac{1}{2\pi} \int_{-\infty}^{\infty} \tilde{p}(k) e^{ik\bar{X}} dk, \tag{3.32}$$

hence, we have

$$p' = \underbrace{-i\alpha_0 \frac{1}{2\pi} \int_{-\infty}^{\infty} \left[\frac{k \int_{\theta V_w}^{\infty} \mathrm{Ai}(s)ds}{\theta^2 \mathrm{Ai}'(\theta V_w) - k^2 \int_{\theta V_w}^{\infty} \mathrm{Ai}(s)ds} e^{ik\bar{X}} \right] dk}_{I_p} + \underbrace{\alpha_0 H(\bar{X})}_{stepfunction}. \tag{3.33}$$

Here the integral I_p represents the induced pressure distribution, which will be calculated upstream when $\bar{X} < 0$, for different cases, in what follows.

[12]Here, recall $\mathcal{F}$ denotes the Fourier transform.

3.3 Plate at rest

To begin the study of upstream influence, we will find the analytic solution for the case when the flat plate is at rest, i.e. when $V_w = 0$. In this case, the integral I_p from (3.33) can be written as

$$I_p = -i\alpha_0 \frac{1}{2\pi} \int_{-\infty}^{\infty} \left[\frac{k \int_0^\infty \mathrm{Ai}(s)ds}{\theta^2 \mathrm{Ai}'(0) - k^2 \int_0^\infty \mathrm{Ai}(s)ds} e^{ik\bar{X}} \right] dk. \tag{3.34}$$

Firstly, we shall make use of the result

$$\int_0^\infty \mathrm{Ai}(s)ds = \frac{1}{3}. \tag{3.35}$$

Hence, (3.34) becomes

$$I_p = -i\alpha_0 \frac{1}{2\pi} \int_{-\infty}^{\infty} \left[\frac{k}{3\theta^2 \mathrm{Ai}'(0) - k^2} e^{ik\bar{X}} \right] dk = -i\alpha_0 \frac{1}{2\pi} \int_{-\infty}^{\infty} \left[\frac{f(k)}{g(k)} \right] dk. \tag{3.36}$$

This integral can be found analytically by Jordan's Lemma, which provides a method to calculate the integral over the real axis by considering the contour integral in the complex plane (see Figurer 3.4) and subsequent use of Cauchy's integral theorem. To calculate the contour integral we require the singularities of the integrand of I_p.

So, we progress by calculating the singularities of the integrand in (3.36), i.e. the zeros of the denominator given by the roots of $g(k) = 0$. Therefore, we have

$$(ik)^{2/3} 3\mathrm{Ai}'(0) - k^2 = 0, \tag{3.37}$$

Note, here we have substituted $\theta = (ik)^{1/3}$. Also, noticing that we can write $i^2 = -1$, we have

$$(ik)^{2/3} 3\mathrm{Ai}'(0) + (ik)^2 = 0. \tag{3.38}$$

Hence, we can re-arrange to find the solution for k, which is given by

$$(ik)^{4/3} = -3\mathrm{Ai}'(0), \tag{3.39}$$

where

$$\mathrm{Ai}'(0) = -\frac{1}{3^{1/3}\Gamma\left(\frac{1}{3}\right)} \approx -0.2588. \tag{3.40}$$

Therefore, if we write $\kappa = ik$, we can see from equation (3.39), since $\mathrm{Ai}'(0)$ is negative, κ is real, and is given by

$$\kappa = \left[3 \left|\mathrm{Ai}'(0)\right|\right]^{3/4}. \tag{3.41}$$

Now, to compute the integral given in (3.36), we apply Jordan's Lemma. Consider the Fourier transform of a function $\Phi(\bar{X})$ given below

$$\int_{-\infty}^{\infty} \Phi(\bar{X}) e^{ik\bar{X}} d\bar{X} = \int_{-\infty}^{\infty} \Phi(\bar{X}) e^{ik_r\bar{X}} e^{-k_i\bar{X}} d\bar{X}, \tag{3.42}$$

where k_r and k_i represent the real and imaginary parts of k, respectively. From (3.42), we see that the perturbations decay exponentially downstream (i.e. $\bar{X} > 0$), if k_i is real and positive. Therefore, in the upstream region where $\bar{X} < 0$, we require k_i to be real and negative for the perturbations to decay exponentially. Thus, we calculate the integral (3.36) (taking into account the branch cut as described on page 28) by closing the contour ($\chi = \bar{\chi}_1 + \chi_2$) in the lower half of the complex plane, as shown in Figure 3.3.

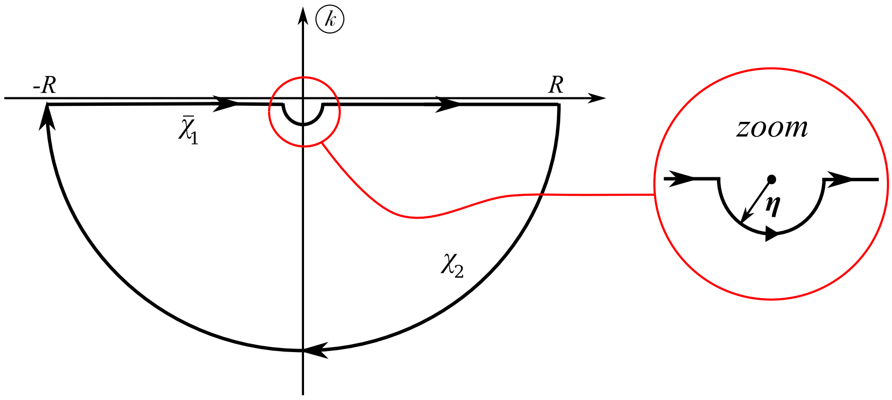

Figure 3.3: Closing the contour in the lower half plane with

From (3.41), we see the singularity $k_0 = -i\kappa$, is purely imaginary, therefore it lies in the lower half of the complex plane on the imaginary axis and is a *simple pole*. This singularity provides the main contribution to the integral in equation (3.34). Now, the integrand is finite at $k = 0$, and tends to zero as $k^{1/3}$. Therefore, as $\eta \to 0$, the path $\bar{\chi}_1$ simply represents the integral over the real line, from $-R$ to R, as shown in Figure 3.4 below. [13]

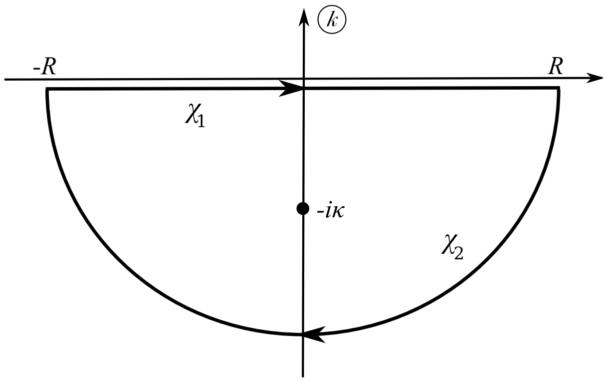

Figure 3.4: To Apply Jordan's Lemma, the contour is closed in the lower half of the complex plane around the singularity $k_0 = -i\kappa$.

To Apply Jordan's Lemma, the contour integral is split over χ_1 and χ_2, hence we have the following

[13] Note, here the contour winds around the singularity in the clockwise direction to preserve the sign of the integral in (3.36).

$$-\oint_{\chi}\left[\frac{k}{3\theta^2\mathrm{Ai}'(0)-k^2}e^{ik\bar{X}}\right]dk=\int_{\chi_1}\left[\frac{k}{3\theta^2\mathrm{Ai}'(0)-k^2}e^{ik\bar{X}}\right]dk-\int_{\chi_2}\left[\frac{k}{3\theta^2\mathrm{Ai}'(0)-k^2}e^{ik\bar{X}}\right]dk. \quad (3.43)$$

Since on χ_1 the variable k is real, thus the first integral on the right hand side of (3.43) is real. As $R\to\infty$ the first integral on the right hand side represents the integral in (3.36), which we wish to find, and since the integrand is *analytic* on χ_2, the second integral on the right hand side disappears by Jordan's Lemma. Thus we calculate the contour integral on the left hand side by utilising Cauchy's Residue Theorem. Since $f(k)$ and $g(k)$ are analytic in the region containing the simple pole k_0, and $f(k_0)\neq 0$, then the integral on the left hand side of (3.43) is given by

$$-\oint_{\chi}\left[\frac{k}{3\theta^2\mathrm{Ai}'(0)-k^2}e^{ik\bar{X}}\right]dk=-2\pi i\mathrm{Res}\left(\frac{f(k)}{g'(k)},k_0\right)=-2\pi i\frac{f(k_0)}{g'(k_0)}. \quad (3.44)$$

Hence, the integral I_p becomes

$$I_p=i\alpha_0\frac{1}{2\pi}\left\{2\pi i\left[\frac{k}{-2i(ik)^{-1/3}\mathrm{Ai}'(0)-2k}e^{ik\bar{X}}\right]\Bigg|_{k=-i\kappa}\right\}. \quad (3.45)$$

So, substituting I_p back into (3.33), the expression for pressure in this case is given by

$$p'=\alpha_0\left[\frac{\kappa}{-2\kappa^{-1/3}\mathrm{Ai}'(0)+2\kappa}e^{\kappa\bar{X}}\right]+\alpha_0H(\bar{X}). \quad (3.46)$$

Since κ is real and positive, and $\mathrm{Ai}'(0)$ is negative, the pressure decays exponentially for $\bar{X}<0$, i.e. upstream of the point where the shock wave impinges on the boundary-layer.

3.4 Plate moving in the downstream direction

Now, let us investigate the effect in the boundary-layer when $V_w>0$. Here we will consider two cases in the analysis of the pressure distribution. First, we shall consider the case for large plate speed, as $V_w\to\infty$, and secondly, for small wall speed as $V_w\to 0$. To begin, for $V_w\neq 0$, we recall the expression for pressure given in (3.33)

$$p'=\underbrace{-i\alpha_0\frac{1}{2\pi}\int_{-\infty}^{\infty}\left[\frac{k\int_{\theta V_w}^{\infty}\mathrm{Ai}(s)ds}{\theta^2\mathrm{Ai}'(\theta V_w)-k^2\int_{\theta V_w}^{\infty}\mathrm{Ai}(s)ds}e^{ik\bar{X}}\right]dk}_{I_p}+\alpha_0H(\bar{X}).$$

3.4.1 Large positive wall speed

Analogous to the previous case, to calculate the integral I_p by applying Jordan's lemma, one requires the zeros of the denominator which is given by

$$\theta^2\mathrm{Ai}'(\theta V_w)-k^2\int_{\theta V_w}^{\infty}\mathrm{Ai}(s)ds=0, \quad (3.47)$$

which can be written

$$\mathrm{Ai}'((ik)^{1/3}V_w) + (ik)^{4/3} \int_{(ik)^{1/3}V_w}^{\infty} \mathrm{Ai}(s)ds = 0. \tag{3.48}$$

For large V_w we consider the asymptotic forms of the derivative and integral of the Airy function Ai, as given by the following formulae[14]

$$\mathrm{Ai}'(w) \sim -\frac{1}{2\sqrt{\pi}} w^{1/4} e^{-\zeta} \sum_{j=0}^{\infty} (-1)^j \frac{d_j}{\zeta^j}, \tag{3.49}$$

$$\int_0^w \mathrm{Ai}(s)ds \sim \frac{1}{3} - \frac{1}{2\sqrt{\pi}} w^{-3/4} e^{-\zeta}, \tag{3.50}$$

for large $|w|$, where ζ is given in (3.20) and the coefficients in (3.49) are given by

$$d_0 = c_0 = 1, \qquad d_j = -\frac{6j+1}{6j-1} c_j, \qquad c_j = \frac{\Gamma(3j+\frac{1}{2})}{54^j j! \Gamma(j+\frac{1}{2})}. \tag{3.51}$$

Thus, putting $\bar{\kappa} = ik$, equation (3.48) to leading order can be written

$$\left[-\frac{1}{2\sqrt{\pi}} (\bar{\kappa}^{1/3} V_w)^{1/4} + \bar{\kappa}^{4/3} \frac{1}{2\sqrt{\pi}} (\bar{\kappa}^{1/3} V_w)^{-3/4} \right] e^{-\zeta} = 0. \tag{3.52}$$

Since $e^{-\zeta} \neq 0$, re-arranging the expression in the brackets we obtain

$$-(\bar{\kappa}^{1/3} V_w) + \bar{\kappa}^{4/3} = 0, \tag{3.53}$$

and we find that

$$\bar{\kappa} = V_w. \tag{3.54}$$

Hence, if $V_w > 0$ then $\bar{\kappa}$ is real and positive, thus, in this case we have the simple pole $k_0 = -iV_w$. Therefore we close the contour around the singularity as before, and the integral I_p is calculated using Cacuhy's Residue Theorem, for which we require the derivative of the denominator of the integrand in (3.33), given by

$$\begin{aligned} \frac{d}{dk} \left[\theta^2 \mathrm{Ai}'(\theta V_w) - k^2 \int_{\theta V_w}^{\infty} \mathrm{Ai}(s)ds \right] &= 2\theta\theta' \mathrm{Ai}'(\theta V_w) + \\ + \theta^3 \theta' V_w^2 \mathrm{Ai}(\theta V_w) - 2k \int_{\theta V_w}^{\infty} \mathrm{Ai}(s)ds &+ k^2 V_w \theta' \mathrm{Ai}(\theta V_w). \end{aligned} \tag{3.55}$$

Note, here $\theta' = d\theta/dk$. So, the integral I_p can be calculated as

$$I_p = \left[\frac{-\alpha_0 k \int_{\theta V_w}^{\infty} \mathrm{Ai}(s)ds}{2\theta\theta' \mathrm{Ai}'(\theta V_w) + \theta^3 \theta' V_w^2 \mathrm{Ai}(\theta V_w) - 2k \int_{\theta V_w}^{\infty} \mathrm{Ai}(s)ds + k^2 V_w \theta' \mathrm{Ai}(\theta V_w)} e^{ik\bar{X}} \right] \Bigg|_{k=-iV_w} . \tag{3.56}$$

Note the change in sign, following the contour integration analogous to the case of the stationary plate. Substituting for θ and evaluating at the simple pole we see

[14] Abramowitz & Stegun (1965); see page 448 & 449

$$I_p = \left[\frac{\alpha_0 i V_w \int_{V_w^{4/3}}^{\infty} \mathrm{Ai}(s)ds}{\frac{2}{3}V_w^{-1/3} i\mathrm{Ai}'(V_w^{4/3}) + \frac{1}{3} i V_w^{7/3}\mathrm{Ai}(V_w^{4/3}) + 2iV_w \int_{V_w^{4/3}}^{\infty} \mathrm{Ai}(s)ds + \frac{1}{3} i V_w^{7/3}\mathrm{Ai}(V_w^{4/3})} e^{V_w \bar{X}} \right], \quad (3.57)$$

which can be simplified to

$$I_p = \left[\frac{\alpha_0 V_w \int_{V_w^{4/3}}^{\infty} \mathrm{Ai}(s)ds}{\frac{2}{3}V_w^{-1/3} \mathrm{Ai}'(V_w^{4/3}) + \frac{2}{3} V_w^{7/3}\mathrm{Ai}(V_w^{4/3}) + 2V_w \int_{V_w^{4/3}}^{\infty} \mathrm{Ai}(s)ds} e^{V_w \bar{X}} \right]. \quad (3.58)$$

In the denominator, for large V_w, we see that the middle term dominates. We can write the fraction in terms of the asymptotic expansions of the Airy function given below, and of the integral and its derivative given (3.49) and (3.50).

$$\mathrm{Ai}(w) \sim \frac{1}{2\sqrt{\pi}} w^{-1/4} e^{-\zeta} \sum_{j=0}^{\infty} (-1)^j \frac{c_j}{\zeta^j}, \quad (3.59)$$

where the coefficients c_j and ζ are given in (3.51). Hence, writing

$$\int_{V_w^{4/3}}^{\infty} \mathrm{Ai}(s)ds = \int_0^{\infty} \mathrm{Ai}(s)ds - \int_0^{V_w^{4/3}} \mathrm{Ai}(s)ds, \quad (3.60)$$

and using the result (3.35), to leading order terms I_p becomes

$$I_p \sim \left[\frac{\alpha_0 V_w (2\sqrt{\pi})^{-1} V_w^{-1} e^{-V_w^2 2/3}}{-2(6\sqrt{\pi})^{-1} e^{-V_w^2 2/3} + 2(6\sqrt{\pi})^{-1} V_w^2 e^{-V_w^2 2/3} + (\sqrt{\pi})^{-1} e^{-V_w^2 2/3} e^{V_w \bar{X}}} \right]. \quad (3.61)$$

Since, in the denominator the term of $O(V_w^2)$ dominates for large V_w, we write the pressure distribution as

$$p' \sim \left[\frac{\alpha_0 3 V_w^{-2}}{2} e^{V_w \bar{X}} \right] + \alpha_0 H(\bar{X}). \quad (3.62)$$

Thus, for large V_w, we see the pressure decays exponentially for $\bar{X} < 0$. If $V_w \bar{X} \sim O(1)$ then $\bar{X} \sim V_w^{-1}$. So, as $V_w \to \infty$, the region of influence upstream tends to shrink. Also, as $V_w \to \infty$ the singularity moves further down the negative imaginary axis.

3.4.2 Small positive wall speed

Now, let us consider the integral I_p for small wall speeds. Recall

$$I_p = -i\alpha_0 \frac{1}{2\pi} \int_{-\infty}^{\infty} \left[\frac{k \int_{z_0}^{\infty} \mathrm{Ai}(s)ds}{\theta^2 \mathrm{Ai}'(z_0) - k^2 \int_{z_0}^{\infty} \mathrm{Ai}(s)ds} e^{ik\bar{X}} \right] dk,$$

where we write

$$z_0 = \theta V_w. \quad (3.63)$$

As before, to evaluate the integral we require the singularities of the integrand, given by

$$\theta^2 \mathrm{Ai}'(z_0) + (ik)^2 \int_{z_0}^{\infty} \mathrm{Ai}(s)ds = 0. \tag{3.64}$$

So, as $V_w \to 0$, we assume that $z_0 \ll 1$. Therefore we estimate the derivative of the Airy function and its integral for small z_0. First let us consider the Taylor expansion of the derivative, given as

$$\mathrm{Ai}'(z_0) = \mathrm{Ai}'(0) + \mathrm{Ai}''(0)z_0 + \frac{1}{2}\mathrm{Ai}'''(0)z_0^2 + \ldots, \tag{3.65}$$

using the result $\mathrm{Ai}''(s) = s\mathrm{Ai}(s)$, we see

$$\mathrm{Ai}'(z_0) = \mathrm{Ai}'(0) + \frac{1}{2}\mathrm{Ai}(0)z_0^2 + \ldots. \tag{3.66}$$

Now let us write the integral in (3.64) as

$$\int_{z_0}^{\infty} \mathrm{Ai}(s)ds = \int_{0}^{\infty} \mathrm{Ai}(s)ds - \int_{0}^{z_0} \mathrm{Ai}(s)ds = \frac{1}{3} - z_0 Ai(0), \tag{3.67}$$

hence, neglecting terms of order $O(z_0^2)$, we write equation (3.64) as

$$(ik)^{2/3}\mathrm{Ai}'(0) + (ik)^2 \left(\frac{1}{3} - z_0 Ai(0)\right) = 0. \tag{3.68}$$

Note, for the case $V_w = 0$, i.e $z_0 = 0$, then (3.68) reduces to (3.38), where the singularity lies on the negative imaginary axis. Let us assume, as the speed increases by a small amount, the singularity deviates by Δk, i.e $k \to -i\kappa + \Delta k$. Thus, from (3.68) we have

$$\mathrm{Ai}'(0) + (-i\kappa + i\Delta k)^{4/3} \left(\frac{1}{3} - (-i\kappa + i\Delta k)^{1/3} V_w Ai(0)\right) = 0.$$

Re-writing we obtain

$$\mathrm{Ai}'(0) + (ik)^{4/3}(1 + \frac{i\Delta k}{ik})^{4/3} \left(\frac{1}{3} - (ik)^{1/3}(1 + \frac{i\Delta k}{ik})^{1/3} V_w Ai(0)\right) = 0,$$

and taking the Taylor expansions of $(1 + [i\Delta k/ik])^{1/3}$ and $(1 + [i\Delta k/ik])^{4/3}$, we have

$$\mathrm{Ai}'(0) + (ik)^{4/3}(1 + \frac{4}{3}\frac{i\Delta k}{ik} + O(\Delta k^2)) \left(\frac{1}{3} - (ik)^{1/3}(1 + \frac{1}{3}\frac{i\Delta k}{ik} + O(\Delta k^2))V_w Ai(0)\right) = 0.$$

Expanding the brackets and neglecting terms of order $O(\Delta k^2)$ yields

$$\mathrm{Ai}'(0) + (\frac{(ik)^{4/3}}{3} + \frac{4}{9}(ik)^{1/3} i\Delta k) - ((ik)^{5/3} + \frac{5}{3}(ik)^{2/3} i\Delta k)V_w Ai(0) = 0,$$

hence, re-arranging for Δk we have

$$i\Delta k \approx \frac{|\mathrm{Ai}'(0)| + (ik)^{5/3} V_w Ai(0) - \frac{(ik)^{4/3}}{3}}{\frac{4}{9}(ik)^{1/3} - \frac{5}{3}(ik)^{2/3} V_w Ai(0)}, \tag{3.69}$$

and putting $k = -i\kappa$ as $V_w \to 0$, we see

$$i\Delta k \approx \frac{|\mathrm{Ai}'(0)| + (\kappa)^{5/3} V_w Ai(0) - |\mathrm{Ai}'(0)|}{\frac{4}{9}(\kappa)^{1/3} - \frac{5}{3}(\kappa)^{2/3} V_w Ai(0)} = \frac{(\kappa)^{5/3} V_w Ai(0)}{\frac{4}{9}(\kappa)^{1/3} - \frac{5}{3}(\kappa)^{2/3} V_w Ai(0)} > 0, \quad (3.70)$$

since the denominator is positive for small V_w.

Hence, Δk is small, negative and imaginary, therefore we see the singularity (i.e. the simple pole in this case) moves further down the negative imaginary axis (recall Figure 3.4), and remains on the imaginary axis. So we expect to obtain pressure distribution with similar properties at the case of a stationary plate and of the plate with large positive speed, i.e. exponential decay upstream, but at a quicker rate than for the case of the stationary plate..

3.5 Plate moving in the upstream direction

Now let us consider the case where the plate moves in the upstream direction, against the flow. In this case, we write the integral I_p as follows

$$\begin{aligned} I_p &= -i\alpha_0 \frac{1}{2\pi} \int_{-\infty}^{\infty} \left[\frac{k \int_{-\theta|V_w|}^{\infty} \mathrm{Ai}(s)ds}{\theta^2 \mathrm{Ai}'(-\theta|V_w|) - k^2 \int_{-\theta|V_w|}^{\infty} \mathrm{Ai}(s)ds} e^{ik\bar{X}} \right] dk \\ &= -i\alpha_0 \frac{1}{2\pi} \int_{-\infty}^{\infty} \left[\frac{F(k)}{G(k)} \right] dk. \end{aligned} \quad (3.71)$$

As usual, attempting to evaluate I_p analytically, we consider the singularities of the integrand, given by

$$G(k) = (ik)^{2/3} \mathrm{Ai}'(-\theta|V_w|) - k^2 \int_{-\theta|V_w|}^{\infty} \mathrm{Ai}(s)ds = 0. \quad (3.72)$$

Now, for example, we see the argument of the first term is dependent on k for negative values. So let us consider the case for small k and large negative wall velocity. We see that the first term in (3.72) dominates, the second is negligible, therefore we have

$$(ik)^{2/3} \mathrm{Ai}'(-\theta|V_w|) = 0. \quad (3.73)$$

Therefore, the roots of this equation depend on $\mathrm{Ai}'(-\theta|V_w|) = 0$. However, for large negative argument, we see that the Airy function and its derivative have infinitely many roots (see appendix C), which lie on the real negative axis[15] . Thus, if we denote the zeros of $\mathrm{Ai}'(-\theta|V_w|)$ as a_n', then we see, from (3.73) the the roots are

$$k_0 = 0, \quad k_n = -i \left(\frac{|a_n'|}{|V_w|} \right)^3, \quad (3.74)$$

where $n = 1, 2, 3, \dots$, for which there are infinite solutions. Therefore in this case, the integral I_p, given in (3.71), is represented by an infinite sum with complex properties.

[15]For the zeros of the Airy function, see book by Abramowitz & Stegun, p. 450, and the book by Valleé & Soares (2004), pp. 15-17

Therefore, the integral I_p, for large $|V_w|$ takes the form

$$\alpha_0 \sum_{n=0}^{\infty} \text{Res}\left(\frac{F}{G}, \tilde{k}_n\right), \tag{3.75}$$

say, as infinite singularities are introduced in the complex "k-plane", where above, $\tilde{k}_n$ are the zeros of $G(k)$ for $n = 0, 1, 2, \ldots$.

We see that in the case of an upstream moving plate, the mathematical inversion of the desired pressure becomes far more complicated. However, based on the analysis of the stationary and downstream moving wall, initially we expect the disturbances upstream to die out exponentially. Due the complexity of the problem, to gain some understanding of the affect of the upstream moving wall, one attempts to solve the integral (3.33) numerically, which we see in the following section.

4 Numerical Solution

Before proceeding, let us consider the form in which the pressure p' is written in (3.33) and the integral representing the Fourier inversion. Firstly, we can re-write (3.33) as

$$p' = -\alpha_0 \frac{1}{2\pi} \int_{-\infty}^{\infty} \left[\frac{\theta^3 \int_{\theta V_w}^{\infty} \mathrm{Ai}(s) ds}{\theta^2 \mathrm{Ai}'(\theta V_w) + \theta^6 \int_{\theta V_w}^{\infty} \mathrm{Ai}(s) ds} \right] e^{ik\bar{X}} dk + \alpha_0 H(\bar{X}), \tag{4.1}$$

where we recall $\theta = (ik)^{1/3}$. Here, the derivative of the perturbed displacement function is given by

$$\frac{dA'}{d\bar{X}} = \frac{1}{2\pi} \int_{-\infty}^{\infty} \left[\alpha_0 \frac{\theta^3 \int_{\theta V_w}^{\infty} \mathrm{Ai}(s) ds}{\theta^2 \mathrm{Ai}'(\theta V_w) + \theta^6 \int_{\theta V_w}^{\infty} \mathrm{Ai}(s) ds} \right] e^{ik\bar{X}} dk, \tag{4.2}$$

and finally let us write

$$\Lambda(k) = \frac{\theta^3 I(z_0)}{\theta^2 \mathrm{Ai}'(\theta V_w) + \theta^6 I(z_0)} = \frac{\theta I(z_0)}{\mathrm{Ai}'(\theta V_w) + \theta^4 I(z_0)}, \tag{4.3}$$

where $z_0 = \theta V_w$ and $I(z_0)$ denotes the integral

$$I(z_0) = \int_{z_0}^{\infty} Ai(s) ds. = \frac{1}{3} - \int_{0}^{z_0} Ai(s) ds. \tag{4.4}$$

Now, let us recall the definition of the Fourier transform of a function $\Phi(\bar{X})$, say, which is given by

$$\mathcal{F}[\Phi](k) = \int_{-\infty}^{\infty} \Phi(\bar{X}) e^{-ik\bar{X}} d\bar{X}. \tag{4.5}$$

This can be written as

$$\mathcal{F}[\Phi](k) = \int_{-\infty}^{\infty} \Phi(\bar{X}) \mathrm{cos}(k\bar{X}) d\bar{X} - i \int_{-\infty}^{\infty} \Phi(\bar{X}) \mathrm{sin}(k\bar{X}) d\bar{X}. \tag{4.6}$$

Therefore, we can see that

$$\mathcal{F}[\Phi](-k) = (c.c.) \left\{ \mathcal{F}[\Phi](k) \right\}, \tag{4.7}$$

where $(c.c.)$ denotes the complex conjugate. If we consider the inverse Fourier transform which recovers $f(\bar{X})$ given by

$$\Phi(\bar{X}) = \frac{1}{2\pi} \int_{-\infty}^{\infty} \mathcal{F}[\Phi](k) e^{ik\bar{X}} dk, \tag{4.8}$$

we see it can be written

$$\Phi(\bar{X}) = \frac{1}{2\pi} \int_{-\infty}^{0} \mathcal{F}[\Phi](k) e^{ik\bar{X}} dk + \frac{1}{2\pi} \int_{0}^{\infty} \mathcal{F}[\Phi](k) e^{ik\bar{X}} dk. \tag{4.9}$$

Making the change of "dummy" variable $k = -r$, we have

$$\Phi(\bar{X}) = -\frac{1}{2\pi}\int_{\infty}^{0} \mathcal{F}[\Phi](-r)e^{-ir\bar{X}}dr + \frac{1}{2\pi}\int_{0}^{\infty} \mathcal{F}[\Phi](k)e^{ik\bar{X}}dk. \tag{4.10}$$

Therefore, from (4.7) we see that (4.10) may be written as

$$\Phi(\bar{X}) = \frac{1}{2\pi}\int_{0}^{\infty} (c.c.)\left\{\mathcal{F}[\Phi](r)\right\} e^{-ir\bar{X}}dr + \frac{1}{2\pi}\int_{0}^{\infty} \mathcal{F}[\Phi](k)e^{ik\bar{X}}dk, \tag{4.11}$$

after changing the orientation of the first integral. Hence, writing (4.11) in its real and imaginary parts we see that

$$\begin{aligned}\Phi(\bar{X}) = &\frac{1}{2\pi}\int_{0}^{\infty} \left(\Re\left\{\mathcal{F}[\Phi](r)\right\} - \Im\left\{\mathcal{F}[\Phi](r)\right\}\right)\left[\cos(r\bar{X}) - i\sin(r\bar{X})\right] dr + \\ &+\frac{1}{2\pi}\int_{0}^{\infty} \left(\Re\left\{\mathcal{F}[\Phi](k)\right\} + \Im\left\{\mathcal{F}[\Phi](k)\right\}\right)\left[\cos(k\bar{X}) + i\sin(k\bar{X})\right] dk,\end{aligned} \tag{4.12}$$

which simplifies to the real integral

$$\Phi(\bar{X}) = \frac{1}{\pi}\int_{0}^{\infty} \left[\Re\left\{\mathcal{F}[\Phi](k)\right\}\cos(k\bar{X}) - \Im\left\{\mathcal{F}[\Phi](k)\right\}\sin(k\bar{X})\right] dk. \tag{4.13}$$

From (3.31), we see that $\Lambda(k)$ represents the Fourier transform of the derivative of the displacement function, hence, making use of (4.13) we can write

$$\frac{dA'}{d\bar{X}} = \frac{1}{\pi}\int_{0}^{\infty} \left[\Re\left\{\Lambda(k)\right\}\cos(k\bar{X}) - \Im\left\{\Lambda(k)\right\}\sin(k\bar{X})\right] dk. \tag{4.14}$$

Thus, once the integral in (4.14) is calculated, the pressure p' given in (4.1) (derived from the Ackeret formula) can be found.

4.1 Numerical Procedure

To calculate the integral above, a Fortran code has been written (see Listing D.1 in the appendix), which takes a value for the plate speed V_w denoted by `vw` at the start of the code. First, we note that the integral is calculated for $x \in [\texttt{xmin}, \texttt{xmax}]$, where the interval is divided into `mx` partitions. The interval of integration for the integral in (4.14) extends from zero to `akmax`, reasonably chosen with `nk` partitions. The derivative of the Airy function $\mathrm{A}i'(z_0)$ and the integral $I(z_0)$ are calculated for each step for k, by first solving the coupled equations

$$\begin{aligned} f'(z) &= g(z), \\ g'(z) &= zf(z), \end{aligned} \tag{4.15}$$

which has the solution $f = \mathrm{Ai}(z)$ and $g = \mathrm{Ai}'(z)$. Once these functions are found using a straight line in the z-plane connecting $z = 0$ and $z = z_0$, the integral $I(z_0)$, given in (4.4), is calculated using the trapezoidal rule for numerical integration with `jz` partitions. Once known, $\Lambda(k)$ is calculated for each step of k in the partitioning of the integral, over k.

When Λ is known, the integral in (4.14) is calculated for the range of values of x described above. The integral is calculated using the mid-ordinate rule with `nk` partitions. Then the pressure $\mathtt{p} = p'/\alpha_0$ and corresponding $\bar{X}$ values are saved to a file, where $\mathtt{p} = \mathtt{h} - dA'/d\bar{X}$ and $\mathtt{h} = 0$ for $\bar{X} < 0$ and $\mathtt{h} = 1$ for $\bar{X} > 0$, i.e. `h` represents the step function.

One must note, when deriving the expression for $\tilde{A}$ (the Fourier transform of the displacement function) given in (3.29), we substitute (3.6c) into (3.6a) and then take the Fourier transform, where the interaction law (3.6c) comprises of the derivative of the displacement function plus the Heaviside step function. The reason this is done, is because the Fourier transform of the Heaviside step function is not well defined at $k = 0$, as

$$\mathcal{F}[H](k) = \int_0^\infty H(\bar{X})e^{-ik\bar{X}}d\bar{X} = -\frac{1}{ik}e^{-ik\bar{X}}\bigg|_0^\infty . \tag{4.16}$$

Hence, in the numerical integration of (4.14), we expect a discrepancy on either side of $\bar{X} = 0$. This is managed by taking a *spline interpolation* of a few points before $\bar{X} = 0$ to give a smooth solution of the pressure as $\bar{X} \to 0^-$. The same is done independently on the other side of $\bar{X} = 0$, i.e. as $\bar{X} \to 0^+$. To implement this, a MATLAB code was written (see Listing D.2 in the appendix).

4.1.1 Results

The results for a downstream and upstream moving plate are shown below in Figure 4.1 and Figure 4.2 respectively.

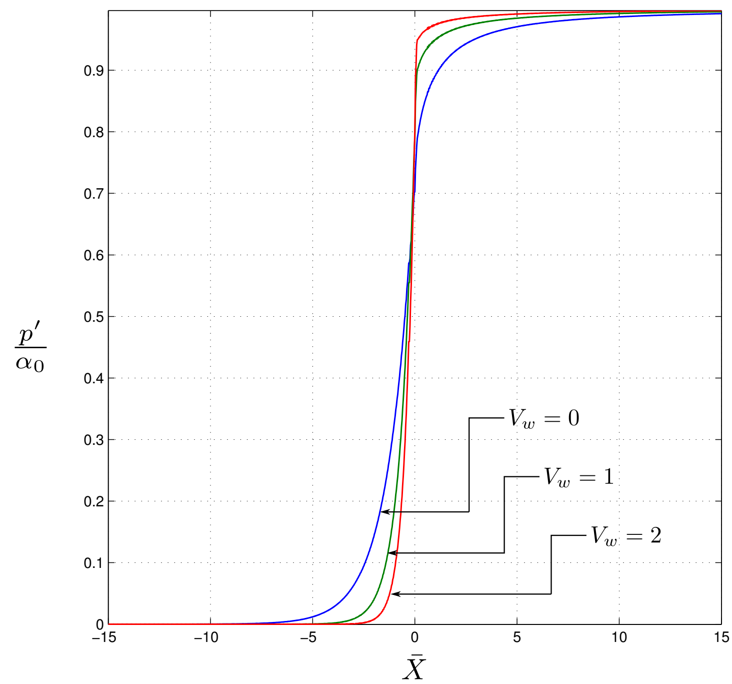

Figure 4.1: Pressure distribution in the interaction region on downstream moving plate.

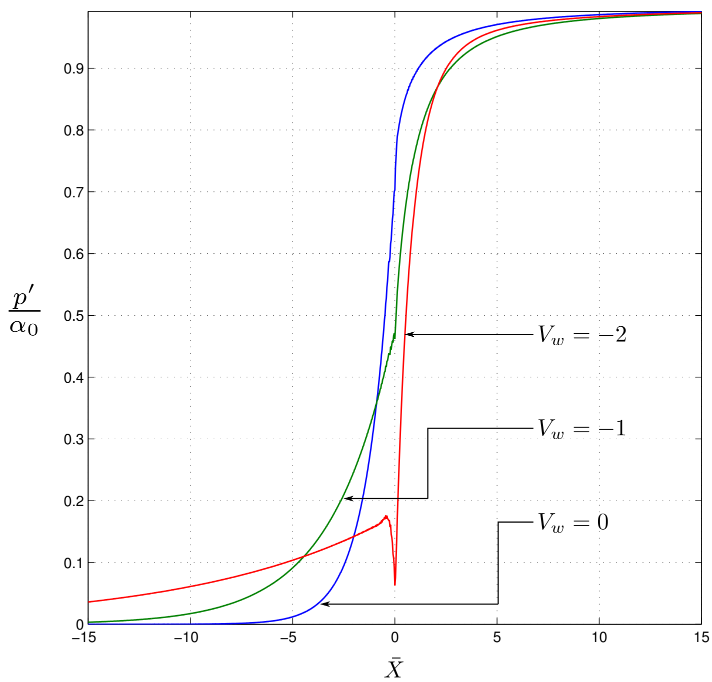

Figure 4.2*:* Pressure distribution in the interaction region on upstream moving plate.

One can see, as the plate speed increases downstream, the region of influence shrinks and the pressure perturbations decay exponentially upstream. When the plate is moving upstream, we see a distinct drop in pressure as $\bar{X} \to 0^-$, which does not converge smoothly with the pressure downstream of the interaction region, whereas in the case of the plate moving in the downstream direction, we see smooth continuation of the pressure. Moreover, a much larger "tail" emerges as $|V_w|$ increases when the plate is moving in the upstream direction, i.e. there is far stronger upstream influence (see Figure 4.2).

5 Conclusions & Further Study

Boundary-layer theory has played a major role in understanding the fluid flow past boundaries such as flat walls, cylinders and aerofoils, and has helped understand the physics of separation. Furthermore, the notion of a boundary-layer has also lead to studies such as the phenomena presented by Liepmann *et al.* via experiments, in which a shockwave impinges on the boundary-layer. Such experiments have provided evidence of upstream disturbances (which otherwise, have thought not to exist) via the agency of the boundary-layer and viscous-inviscid interaction; a process which has significant aerodynamic implications.

In preparation for this study, we started with the Navier-Stokes equations, and understanding the flow in the laminar boundary-layer, from which we construct a triple-deck model (first introduced by Stewartson and Nieland, independently in 1969) in the vicinity of the interaction region. Using the method of matched asymptotic expansions of the solution, we arrive at equations (2.91) - the boundary-layer equations, where the pressure is determined by the interaction-law derived from the Ackeret formula. Through linearisation of the governing equations and the method of Fourier transform, we examined the extent of the upstream influence by seeking the solution for the pressure distribution.

Examining the case of the stationary plate by first seeking the solution to (3.6b), by applying Jordan's lemma, the solution could be found analytically given in (3.46), which decays exponentially upstream. Remarkably a similar result for transverse velocity was found by Lighthill (1953), in his second paper on upstream influence, before triple-deck theory was developed. In the case of the plate moving in the downstream direction, with the use of the asymptotic expansion of the Airy function, we found that the pressure decays exponentially at a greater rate over a region $\bar{X} \sim 1/V_w$. Hence, the region of influence shrinks as plate speed is increased.

It was hoped that the solution could be found analytically, for arguably the more interesting case, where the plate moves in the upstream direction. However, the complexity of (3.71) due to the infinitely many singularitiets given by (3.72) as $V_w \to -\infty$, one resorts to the numerical solution of (3.71). Nevertheless, following the analysis this task is not straightforward, as explained in the previous section, due to the involvement of Dirac delta function in the equation (3.8a). From the numerical solution, we find two very interesting phenomena. Firstly, we see the decay of pressure is much shallower, and as the plate speed increases, the decay seems more algebraic. Secondly, and more interestingly, at the point where the shockwave impinges on the boundary-layer, we see the pressure distribution on either side of this point doesn't converge smoothly in the boundary-layer. Whether this process leads to a discontinuity still remains to be seen, however, one can see the solution no longer remains smooth in the interaction region.

It would be interesting to see how the solution develops for larger values of plate speed. Due to limitations of the code developed, numerical solution was limited. Also, to combat the issue regarding the use of Fourier transform of the generalised function, the Dirac delta function, one could replace the step function given in (1.15) with a function of the kind $\tanh(x/\epsilon)$, say. Here ϵ is a small parameter controlling the smooth increase of pressure over a small distance, much smaller than the length of the interaction region. This may result in "nicer" mathematics as the Fourier transform of hyperbolic tangent is well defined, however, it does not detract from the analysis presented here (see appendix E).

Since, in the case for the upstream moving plate, the solution no longer decays exponentially, it may be better to introduce new scaling for the region upstream of the interaction region. Matching the solution upstream (long scale) asymptotically with the solution in the interaction region (short scale), may gain an insightful model for the pressure distribution in the upstream region where a long "tail" emerges, as seen in Figure 4.2. Reasoning for this approach relates to the relevant fluid forces in different regions. Let us consider the upstream region as the "outer" region and the interaction region as the "inner" region. In the inner region, due to the abrupt change in pressure, the viscous terms are not important and we apply the Ackeret formula. However, in the outer region the pressure terms may not dominate and one expects viscous dissipation to play an important role. In the interaction region, ideally, one would like to find an analytic solution to (3.71). Finally, the numerical results obtained for the upstream moving wall suggests that the displacement of the of the boundary-layer experiences large variation in the interaction region, whether this result is physical requires further analysis. Ergo, we find upstream influence still poses interesting questions in the 21$^{\text{st}}$ century!

A Nomenclature

x, y	non-dimensional longitudinal and normal coordinates, respectively
u, v	non-dimensional longitudinal and normal components of velocity
p, ρ, μ, h	non-dimensional pressure, density, dynamic viscosity and enthalpy
$A_1(x_*)$	the boundary-layer displacement function
a_∞	free stream speed of sound
α_0	parameter which controls strength of the shock
$(')$	denotes the perturbations of the solution when linearising, unless stated otherwise
$(\hat{\ })$	denotes the variables and solutions in dimensional form
$(^-)$	denotes the variables and solutions in canonical form
$(\tilde{\ })$	denotes the Fourier transform of the solutions
$(\breve{\ })$	denotes asymptotic expansion of solutions in the middle tier
$(_w)$	denotes the condition at the boundary surface/plate/wall
γ	gas constant given by ratio of specific heats of the gas
δ, δ_i	the displacement of the streamlines in the boundary-layer
$\mathcal{F}[f](k)$	denotes Fourier transform of function f with transform variable k
λ	denotes the non-dimensional skin friction on the boundary surface
M_∞	the free stream Mach number
ψ^*	denotes the stream function in the viscous sublayer
Pr	denotes the Prandtl number
Re	denotes the Reynolds number
Θ	the slop angle of the stream lines in the boundary-layer
V_∞	free stream velocity
V_w	boundary surface/wall/plate velocity

B Essence of Asymptotic Expansions

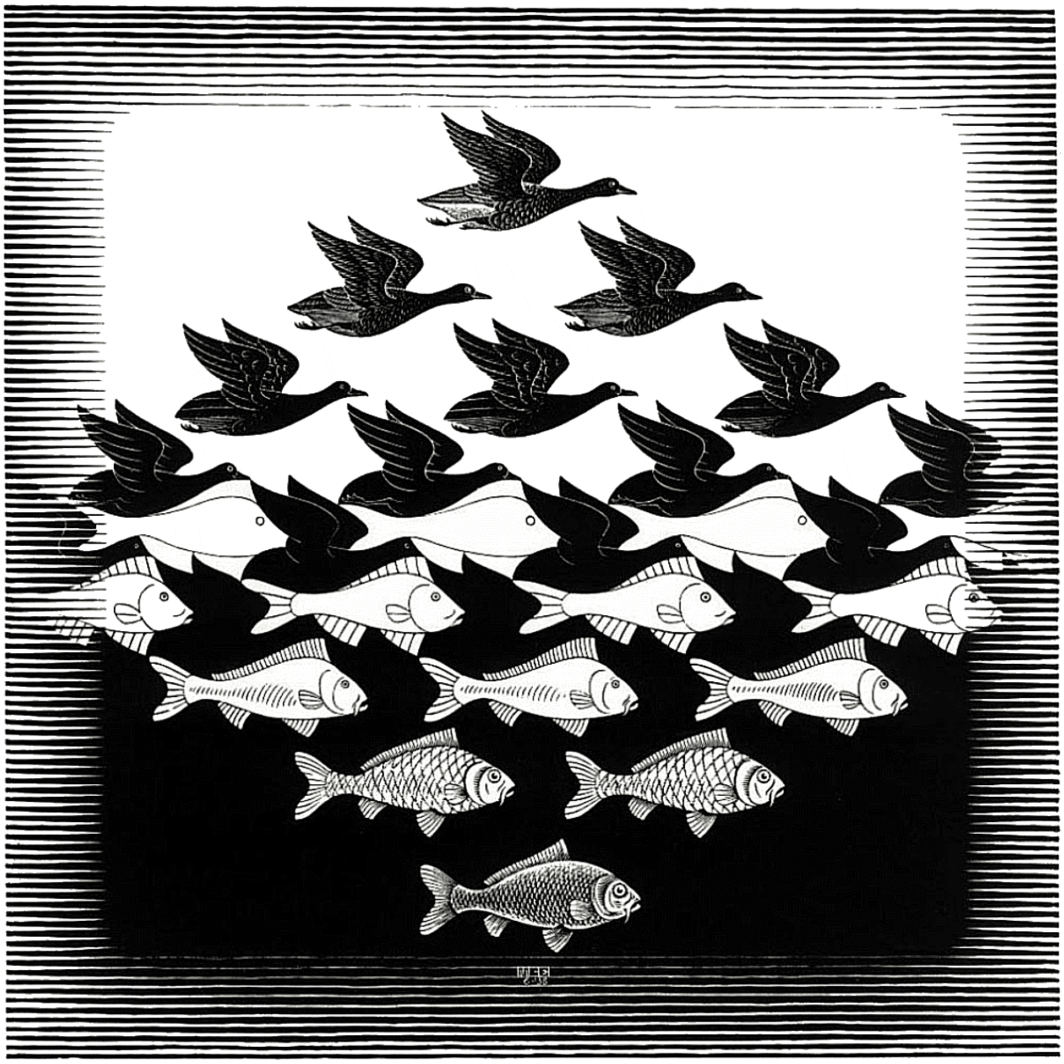

Figure B.1: SKY AND WATER I (1938) by M. C. Escher

Considering this woodcut by the Dutch artist M. C. Escher[16], one can get a feeling for the method of matched asymptotic expansions. In this piece, we see a smooth blending from the bottom to the top, which essentially describes the smooth continuation of the solution from one region to another, such as those presented in the triple-deck model (see page 15).

[16]As seen in the book by Van Dyke (1964).

C Airy Function

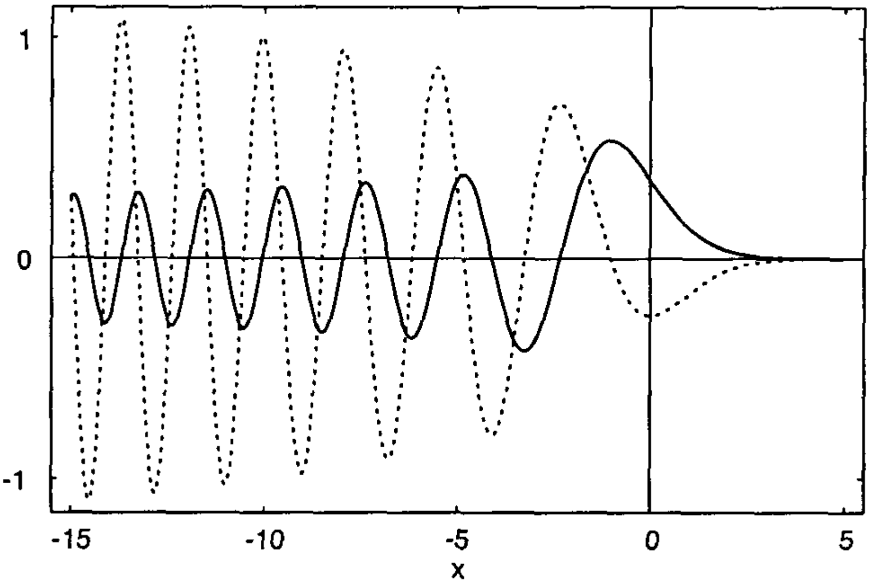

Figure C.1: Airy function Ai(x) -*solid*, and its derivative Ai$'$(x) - *dashed*. See book by Valleé & Soares (2004) p. 17

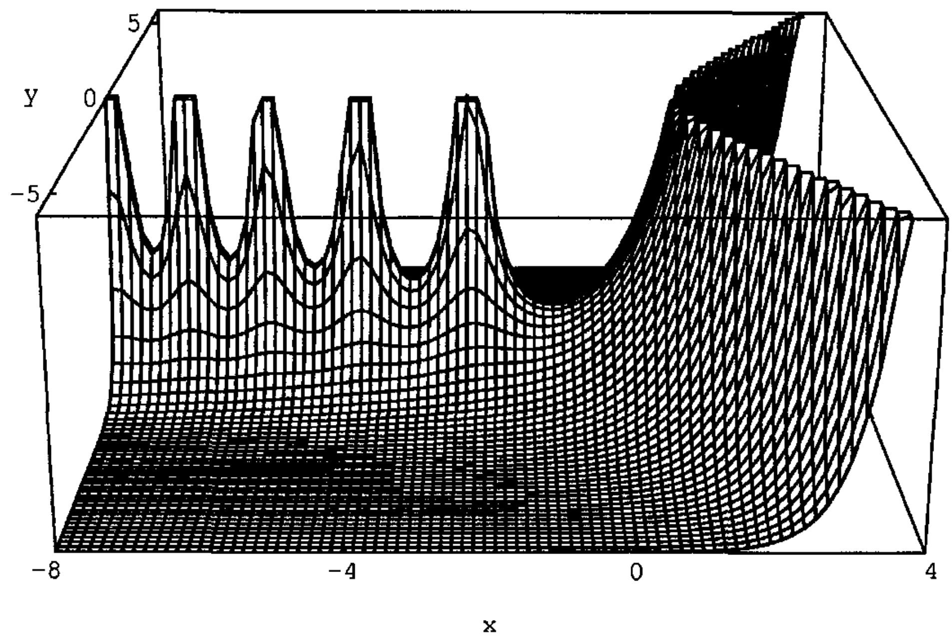

Figure C.2: Airy function Ai(x) Plot of $1/|\mathrm{Ai}(z)|$. Zeros of $|Ai(z)|$ are located on the negative part of the real axis. See book by Valleé & Soares (2004) p. 17

D Source Code

Listing D.1: Fortran code used to calculate pressure distribution.

```
PROGRAM MOVINGPLATE

REAL :: pi, dk, ak, dx, x, ax, h, p
COMPLEX :: ci, t, z0, dz, z1, z2, cint
REAL, PARAMETER :: vw=-2., xmax=15., xmin=-15., akmax=3000.
INTEGER, PARAMETER :: mx=1000, nk=30000, jz=1000
COMPLEX :: f(0:jz), g(0:jz), cf(1:nk)

!data is saved in new file.
OPEN (10, FILE='pdash2u.dat')

 ci=CMPLX(0.,1.)
 pi=4.*ATAN(1.)
 dk=akmax/nk
 !dk represents the step size used in order to compute the
 !integral for variable vw.
DO l=1,nk
   ak=dk*l-dk/2.
   t=(ak**(1./3.))*(SQRT(3.)+ci)/2. !=(ik)^(1/3)
   z0=t*vw
   dz=z0/jz
   f(0)=CMPLX(.355028,0.)
   g(0)=CMPLX(-.258819,0.)
   !below, the Airy function and its derivative are computed by
   !solving the Airy equation as coupled ode with step dz.
   DO j=1,jz
      f(j)=f(j-1)+(dz*g(j-1))
      z1=dz*(j-1)
      g(j)=g(j-1)+(dz*z1*f(j-1))
      f(j)=f(j-1)+(dz*(g(j)+g(j-1))/2.)
      z2=dz*j
      g(j)=g(j-1)+(dz*(z2*f(j)+z1*f(j-1))/2.)
   END DO
   cint=CMPLX(.333333,0.)
   !integral of Airy function from zero to infinity = 1/3.
   DO j=1,jz
      cint=cint-(dz*(f(j)+f(j-1))/2.)
   END DO
   !above, the integral of the Airy function from z0 to infinity
   !is computed using the trapezoidal rule for numerical
```

```
   !integration. Recall the integral can be writted as the
   !integral from zero to infinity minus the integral from
   !zero to z0.
   cf(l)=(t*cint)/(g(jz)+((t**4)*cint))
END DO

!below, the pressure distribution is computed between xmin and
!xmax, either side
!of the interaction region.
dx=(xmax-xmin)/mx
DO j=0,mx
   x=xmin+dx*j
   ax=0.
   DO  l=1,nk
      ak=(dk*l)-(k/2.)
      ax=ax+(dk*(REAL(cf(l))*COS(ak*x)-AIMAG(cf(l))*SIN(ak*x))/pi)
   END DO
   !above, the integral representing the derivative of the
   !displacement function is computed from k=0 to some sufficently
   !large number, here we choose akmax=3000.
   h=0.
   IF(x>0.)h=1.
   p=h-ax
   !here we stick with the step function of pressure increase due
   !to the shock.
   WRITE(10,'(2F12.6)') x, p
   !results are written to the new file created.
END DO

CLOSE(10)

END PROGRAM MOVINGPLATE
```

Listing D.2: Spline code in MATLAB - used to resolve issue in Fourier space.

```
function [newdata]=splinepoints(data)
[a,~]=size(data);
b=0;
for i=1:a
    if(data(i,1)>=0.)
        b=1;
        c=i;
    end
    if(b==1)
        break
    end
end

xx1=linspace(data(c-10,1),data(c-2,1),10);
yy1=spline(data(c-10:c-2,1),data(c-10:c-2,2),xx1);
data(c-9:c,2)=yy1;

xx2=linspace(data(c+1,1),data(c+10),10);
yy2=spline(data(c+1:c+10,1),data(c+1:c+10,2),xx2);
data(c+1:c+10,2)=yy2;

newdata=data;
```

E Smooth imposed pressure variation in the interaction region

Here, we consider a function which varies smoothly over a small region ($\bar{\epsilon}$, say, much smaller than the extent of the interaction region), opposed to the step function used to describe the increase in pressure due to the shock wave. In this case, the imposed pressure could for example take the form

$$\bar{p}_0 = \frac{1}{2}\left(\tanh(\bar{X}/\bar{\epsilon}) + 1\right), \tag{E.1}$$

so there is a "sharp" but smooth variation from $\bar{p}_0 = 0$ to $\bar{p}_0 = 1$ in the vicinity of $\bar{X} = 0$.

Thus, equations (3.8) become

$$(\bar{Y} + V_w)\frac{\partial u'}{\partial \bar{X}} + v' = \frac{d^2 A'}{d\bar{X}^2} - \frac{1}{2\bar{\epsilon}}\text{sech}^2(\bar{X}/\bar{\epsilon}) + \frac{\partial^2 u'}{\partial \bar{Y}^2}, \tag{E.2a}$$

$$\frac{\partial u'}{\partial \bar{X}} + \frac{\partial v'}{\partial \bar{Y}} = 0. \tag{E.2b}$$

Taking the Fourier transform of (E.2) (noting the Fourier transform of sech^2 is well defined), we have[17]

$$(\bar{Y} + V_w)ik\tilde{u} + \tilde{v} = -k^2\tilde{A} - \bar{\epsilon}k\sqrt{\frac{\pi}{2^3}}\text{cosech}(\pi k/2) + \frac{d^2\tilde{u}}{d\bar{Y}^2}, \tag{E.3a}$$

$$ik\tilde{u} + \frac{d\tilde{v}}{d\bar{Y}} = 0. \tag{E.3b}$$

So, equation (3.16) still holds and the required third boundary condition (3.17c) becomes

$$\frac{d^2\tilde{u}}{d\bar{Y}^2} = k^2\tilde{A} + \bar{\epsilon}k\sqrt{\frac{\pi}{2^3}}\text{cosech}(\pi k/2) \qquad \text{at} \qquad \bar{Y} = 0, \tag{E.4}$$

and C_1 from (3.24) becomes

$$C_1 = \frac{k^2\tilde{A} + \bar{\epsilon}k\sqrt{\frac{\pi}{2^3}}\text{cosech}(\pi k/2)}{\theta^2\text{Ai}'(\theta V_w)}. \tag{E.5}$$

Now, following the analysis as before to gain the second relationship between the constant C_1 and $\tilde{A}$ in (3.28), and subsequently eliminating C_1 using (E.5), we find that

$$\tilde{A} = \frac{\bar{\epsilon}k\sqrt{\frac{\pi}{2^3}}\text{cosech}(\pi k/2)\int_{\theta V_w}^{\infty}\text{Ai}(s)ds}{\theta^2\text{Ai}'(\theta V_w) - k^2\int_{\theta V_w}^{\infty}\text{Ai}(s)ds}. \tag{E.6}$$

[17]Here $\mathcal{F}[\text{sech}^2(x)](k) = k(\sqrt{\pi/2})\text{cosech}(\pi k/2)$.

Hence, we obtain

$$\tilde{p} = -i \frac{\bar{\epsilon} k \sqrt{\frac{\pi}{2^3}} \operatorname{cosech}(\pi k/2) \int_{\theta V_w}^{\infty} \mathrm{Ai}(s) s}{\theta^2 \mathrm{Ai}'(\theta V_w) - k^2 \int_{\theta V_w}^{\infty} \mathrm{Ai}(s) ds} + \mathcal{F}\left[\frac{1}{2}\left(\tanh(\bar{X}/\bar{\epsilon}) + 1\right)\right](k). \tag{E.7}$$

Finally, we have

$$p' = -i \frac{1}{2\pi} \int_{-\infty}^{\infty} \left[\frac{\bar{\epsilon} k \sqrt{\frac{\pi}{2^3}} \operatorname{cosech}(\pi k/2) \int_{\theta V_w}^{\infty} \mathrm{Ai}(s) ds}{\theta^2 \mathrm{Ai}'(\theta V_w) - k^2 \int_{\theta V_w}^{\infty} \mathrm{Ai}(s) ds} e^{ik\bar{X}}\right] dk + \frac{1}{2}\left(\tanh(\bar{X}/\bar{\epsilon}) + 1\right). \tag{E.8}$$

So, with the luxury of time, one could compute the integral in (E.8) numerically and compare with the results found in section 4.1.1, since in the above the issue regarding the singularity in the Fourier transform of the Heaviside step function at $k = 0$ has been resolved by choosing $\bar{p}_0$ as in (E.1).

Therefore, the numerical results of (E.8) could provide further insight on the "kick" in pressure found in Figure 4.2, and thus also the pressure either side of $\bar{X} = 0$ (where the shock wave impinges on the boundary-layer).

References

[Abramowitz & Stegun, 1965] Abramowitz, M., Stegun, I. A., 1965. *Handbook of Mathematical Functions.* 3rd edn. New York: Dover Publications Inc.

[Chapman *et al.*, 1956] Chapman, D. R., Kuehn, D. M. & Larson, H. K., 1956. Investigation of separated flows in supersonic and subsonic streams with emphasis on the effect of transition. *National Advisory Committee for Aeronautics*, Washington, D. C, **1356**, pp. 421-460.

[Goldstein, 1948] Goldstein, S., 1948. On laminar boundary-layer flow near a position of separation. *Q. J. Mech. Appl. Math.*, **1**, pp. 4369.

[Kaplun, 1967] Kaplun, S. 1988. *Fluid Mechanics and Singular Perturbations.* P. A. Lagerstrom, L. N. Howard, C. S. Liu (eds.). New York: Academic Press.

[Lagerstrom, 1988] Lagerstrom, P. A., 1988. *Matched Asymptotic Expansions: Ideas and Techniques.* New York: Springer-Verlag. pp. 27-29.

[Liepmann *et al.*, 1949] Liepmann, H. W., Roshko, A., Dhawan, S., 1949. On Reflection of Shock Waves from Boundary Layers. *National Advisory Committee for Aeronautics*, Washington, D. C, **2334** (1951), pp. 887-917.

[Liepmann & Roshko, 1957] Liepmann, H. W., Roshko, A., 1957. *Elements of Gas Dynamics.* New York: John Wiley & Sons, Inc. pp. 109-110.

[Lighthill, 1953] Lighthill, J., 1953. On Boundary Layers and Upstream Influence. II. Supersonic Flows without Separation *Proc. R. Soc. Lond.*, **A 217 1131**, pp. 478-507

[Lighthill, 2000] Lighthill, J., 2000. Upstream influence in boundary layers 45 years ago. *Phil. Trans. R. Soc. Lond.*, **A 358 1777**, pp. 30473061

[Nieland, 1969] Neiland, V. Y., 1969. Upstream influence in boundary layers 45 years ago. *Izv. Akad. Nauk SSSR, Mech. Zhidk. Gaza*, **4**, pp. 5357.

[Oswatitsch & Wieghardt, 1948] Oswatitsch, K., Wieghardt, K., 1948. Theoretical analysis of stationary potential flows and boundary layers at high speed. *NACA Tech. Memo.*, **1189**.

[Rogers, 1992] Rogers, D. F., 1992. *Laminar Flow Analysis.* New York: Cambridge University Press.

[Schlichting, 2000] Schlichting, H., Gersten, K., 2000. *Boundary-Layer Theory.* 8th ed. Berlin: Springer.

[Stewartson, 1951] Stewartson, K., 1951. On the interaction between shock waves and boundary layers. *Mathematical Proceedings of the Cambridge Philosophical Society*, **47**, pp. 545-553

[Stewartson, 1964] Stewartson, K., 1964. *The Theory Of Laminar Boundary Layers In Compressible Fluids.* London: Oxford University Press.

[Stewartson, 1974] Stewartson, K., 1974. Multi-structured boundary layers on flat plates and related bodies. *Adv. Appl Mech.*,**14**, pp.145-239.

[Stewartson & Williams, 1969] Stewartson, K., Williams, P. G., 1969. Self-induced separation. *Proc. Roy. Soc. Lond.*, **A 312**, pp. 181206.

[Sychev *et al.*, 1998] Sychev, V. V., Ruban A. I., Sychev, V. V., Korolev, G. L., 1998. *Asymptotic Theory of Separated Flows.* Cambridge University Press: New York. pp. 9-99

[Valleé & Soares, 2004] Valleé, O., Soares, M., 2004. *Airy Functions And Applications To Physics.* Imperial College Press: London.

[Van Dyke, 1964] Van Dyke, M., 1964. *Perturbation methods in fluid mechanics.* Academic Press: New York .